Inverse Problems **28** (2012) 085009 (38pp) doi:10.1088/0266-5611/28/8/085009

A linearized inverse scattering problem for the polarized waves and anisotropic targets

Mikhail Gilman, Erick Smith and Semyon Tsynkov

Department of Mathematics, North Carolina State University, Campus Box 8205, Raleigh, NC 27695, USA

E-mail: tsynkov@math.ncsu.edu

Received 1 February 2012, in final form 26 June 2012
Published 17 July 2012
Online at stacks.iop.org/IP/28/085009

Abstract

We analyze the scattering of a plane transverse linearly polarized electromagnetic wave off a plane interface between the vacuum and a given material. For a variety of predominantly dielectric materials, from isotropic to anisotropic and weakly conductive, we show that when the scattering is weak, the first Born approximation predicts the correct scattered field in the vacuum region. We also formulate and solve the corresponding linearized inverse scattering problem. Specifically, we provide a necessary and sufficient condition under which interpreting the target material as a weakly conductive uniaxial crystal allows one to reconstruct all the degrees of freedom contained in the complex 2×2 Sinclair scattering matrix. This development can help construct a full-fledged radar ambiguity theory for polarimetric imaging by means of a synthetic aperture radar (SAR), which is in contrast to the approach that currently dominates the SAR literature and exploits a fully phenomenological scattering matrix. Moreover, the linearized scattering off a material half-space naturally gives rise to the ground reflectivity function in the form of a single layer (i.e. a δ-layer) at the interface. A ground reflectivity function of this type is often introduced in the SAR literature without a rigorous justification. Besides the conventional SAR analysis, we expect that the proposed approach may appear useful for the material identification SAR (miSAR) purposes.

(Some figures may appear in colour only in the online journal)

1. Background

1.1. Direct and inverse scattering problems

Maxwell's equations of electromagnetism in CGS units [1, 2]:

$$\frac{1}{c}\frac{\partial \boldsymbol{H}}{\partial t} + \nabla \times \boldsymbol{E} = 0, \quad \nabla \cdot \boldsymbol{H} = 0,$$
$$\frac{1}{c}\frac{\partial \boldsymbol{D}}{\partial t} - \nabla \times \boldsymbol{H} = -\frac{4\pi}{c}(\boldsymbol{j} + \boldsymbol{j}^{(\mathrm{ex})}), \quad \nabla \cdot \boldsymbol{D} = 0, \tag{1}$$

govern the electromagnetic field driven by the extraneous electric current with the density $\boldsymbol{j}^{(\mathrm{ex})} = \boldsymbol{j}^{(\mathrm{ex})}(\boldsymbol{x}, t)$. In the system (1), c is the speed of light in vacuum, $\boldsymbol{E}$ and $\boldsymbol{H}$ denote the vectors of the electric and magnetic field, respectively, and $\boldsymbol{D}$ is the vector of electric induction, which is related to the electric field via the permittivity tensor $\boldsymbol{\varepsilon} = \boldsymbol{\varepsilon}(\boldsymbol{x})$ (hereafter, the dot '$\cdot$' denotes the tensor convolution):

$$\boldsymbol{D} = \boldsymbol{\varepsilon} \cdot \boldsymbol{E}. \tag{2}$$

The total current in the system (1) is a sum of $\boldsymbol{j}^{(\mathrm{ex})}$ and the conductivity current $\boldsymbol{j}$ given by

$$\boldsymbol{j} = \boldsymbol{\sigma} \cdot \boldsymbol{E}. \tag{3}$$

The quantity $\boldsymbol{\sigma}$ in (3) denotes the conductivity tensor, which may also vary in space: $\boldsymbol{\sigma} = \boldsymbol{\sigma}(\boldsymbol{x})$. We are assuming that the current $\boldsymbol{j}^{(\mathrm{ex})}$ does not lead to the accumulation of the extraneous electric charge, so that the second steady-state equation in the system (1) (the Gauss law of electricity) is homogeneous. The magnetic permeability is assumed equal to 1 (for the range of phenomena of interest) so that there is no need to distinguish between the magnetic field and magnetic induction.

Let $\boldsymbol{E}^{(\mathrm{inc})}$ and $\boldsymbol{H}^{(\mathrm{inc})}$ denote the incident fields that satisfy the system (1) in vacuum:

$$\begin{aligned} &\frac{1}{c}\frac{\partial \boldsymbol{H}^{(\mathrm{inc})}}{\partial t} + \nabla \times \boldsymbol{E}^{(\mathrm{inc})} = \boldsymbol{0}, \qquad \nabla \cdot \boldsymbol{H}^{(\mathrm{inc})} = 0, \\ &\frac{1}{c}\frac{\partial \boldsymbol{E}^{(\mathrm{inc})}}{\partial t} - \nabla \times \boldsymbol{H}^{(\mathrm{inc})} = -\frac{4\pi}{c}\boldsymbol{j}^{(\mathrm{ex})}, \qquad \nabla \cdot \boldsymbol{E}^{(\mathrm{inc})} = 0. \end{aligned} \tag{4}$$

Then, the total fields that solve (1) can be represented as

$$\boldsymbol{E} = \boldsymbol{E}^{(\mathrm{inc})} + \boldsymbol{E}^{(\mathrm{sc})} \quad \text{and} \quad \boldsymbol{H} = \boldsymbol{H}^{(\mathrm{inc})} + \boldsymbol{H}^{(\mathrm{sc})}, \tag{5}$$

where the corrections $\boldsymbol{E}^{(\mathrm{sc})}$ and $\boldsymbol{H}^{(\mathrm{sc})}$ shall be attributed to the variation of $\boldsymbol{\varepsilon}$ and $\boldsymbol{\sigma}$ against the background vacuum values $\boldsymbol{\varepsilon} = \mathcal{I}$ (identity tensor) and $\boldsymbol{\sigma} = \boldsymbol{0}$, respectively. Those corrections are referred to as the scattered fields. The direct electromagnetic scattering problem is the problem of determining the scattered fields $\boldsymbol{E}^{(\mathrm{sc})}$ and $\boldsymbol{H}^{(\mathrm{sc})}$ if $\boldsymbol{\varepsilon} = \boldsymbol{\varepsilon}(\boldsymbol{x})$ and $\boldsymbol{\sigma} = \boldsymbol{\sigma}(\boldsymbol{x})$ are given. The inverse electromagnetic scattering problem rather consists in determining the variable electric permittivity $\boldsymbol{\varepsilon} = \boldsymbol{\varepsilon}(\boldsymbol{x})$ and conductivity $\boldsymbol{\sigma} = \boldsymbol{\sigma}(\boldsymbol{x})$ under the assumption that the scattered fields $\boldsymbol{E}^{(\mathrm{sc})}$ and $\boldsymbol{H}^{(\mathrm{sc})}$ are available. The region of space where $\boldsymbol{\varepsilon} = \boldsymbol{\varepsilon}(\boldsymbol{x})$ and $\boldsymbol{\sigma} = \boldsymbol{\sigma}(\boldsymbol{x})$ are to be reconstructed is called the target. The inverse scattering problem may have multiple solutions.

1.2. The first Born approximation

In the literature, the foregoing scattering problems are often studied using second-order governing equations for the individual fields. Moreover, the inverse scattering problem can be simplified by means of the linearization based on the first Born approximation; see [3, chapter XIII]. It is typically used when the scattered field is much smaller than the incident field, i.e. when the scattering is weak. This, in turn, can be expected to be the case when the deviation of the material parameters at the target from the background parameters in vacuum is small. In Appendix A, we show that when the target material is isotropic, i.e. when both the permittivity and conductivity tensors are spherical, the governing equation for the scattered electric field under the first Born approximation becomes (see equation (A.8))

$$\frac{1}{c^2}\frac{\partial^2 \boldsymbol{E}^{(\mathrm{sc})}}{\partial t^2} - \Delta \boldsymbol{E}^{(\mathrm{sc})} = \nu \frac{\partial^2 \boldsymbol{E}^{(\mathrm{inc})}}{\partial t^2} - \frac{4\pi\sigma}{c^2}\frac{\partial \boldsymbol{E}^{(\mathrm{inc})}}{\partial t}, \tag{6}$$

where the scalar quantity ν is the ground reflectivity function (see formula (A.7)):

$$\nu(\boldsymbol{x}) = \frac{1}{c^2} - \frac{1}{v(\boldsymbol{x})^2}. \tag{7}$$

In formula (7), $v = v(\boldsymbol{x})$ is the local propagation speed in the material. More rigorously, a solution by means of the first Born approximation can be obtained by truncating the corresponding Neumann series after its linear term [4, chapter 6].

In the literature, the Born approximation is often discussed along with another approximation, named after Rytov; see, e.g., [3, chapter XIII] and [5, 6]. It is known that the Rytov approximation better describes the transmitted waves, i.e. the field inside the target material, whereas the Born approximation is better suited for the reflected waves, i.e. for the scattered field in vacuum (see, e.g., [6, 7] and references therein). We will focus on the first Born approximation for the rest of this paper, because it provides a linearized scattering model for the field reflected off the target into the vacuum region, which is convenient for SAR applications.

We also note that in the Cartesian coordinates, the vector equation (6) decouples into three independent scalar wave equations for the individual field components. This enables studying the scattering problems in the scalar formulation [8], provided that the polarization of the field is either not important or not detected by the specific equipment.

1.3. Scalar versus polarimetric SAR

Many currently operating SAR sensors use linear chirps

$$P(t) = A(t)\,\mathrm{e}^{\mathrm{i}\omega_0 t}, \quad \text{where} \quad A(t) = \chi_\tau(t)\,\mathrm{e}^{\mathrm{i}\alpha t^2}, \tag{8}$$

as interrogating waveforms [8]. In formula (8), ω_0 is the carrier frequency, $\chi_\tau(t)$ is the indicator function of the interval $[-\tau/2, \tau/2]$ and the modulating function $A(t)$ varies slowly compared to the fast oscillation $\mathrm{e}^{\mathrm{i}\omega_0 t}$.

Let us first disregard the polarization and identify pulse (8) with the right-hand side of the scalar counterpart of equation (A.5). This right-hand side shall be interpreted as the time derivative of a given Cartesian component of the electric current at the emitting SAR antenna, which is taken as a point source[1] located at $\boldsymbol{x} \in \mathbb{R}^3$. Then, the corresponding component of the incident field due to the emitted chirp (8) is given by the standard retarded potential of the d'Alembert operator:

$$E^{(\mathrm{inc})}(\boldsymbol{z}, t) = \frac{1}{4\pi} \frac{P(t - |\boldsymbol{z} - \boldsymbol{x}|/c)}{|\boldsymbol{z} - \boldsymbol{x}|}. \tag{9}$$

When substituting $E^{(\mathrm{inc})}$ of (9) into the right-hand side of equation (6), we can leave $A(\,\cdot\,)$ out of the differentiation w.r.t. t, because $A(\,\cdot\,)$ varies slowly. Subsequently, a solution of equation (6) can be obtained with the help of the Kirchhoff integral. In particular, the scattered field back at the antenna $\boldsymbol{x}$ is given by the following expression:

$$\begin{aligned} E^{(\mathrm{sc})}(\boldsymbol{x}, t) &\approx -\frac{\omega_0^2}{16\pi^2} \iiint_{|\boldsymbol{x}-\boldsymbol{z}| \leqslant ct} \frac{\hat{\nu}(\boldsymbol{z})}{|\boldsymbol{x} - \boldsymbol{z}|^2} P(t - 2|\boldsymbol{x} - \boldsymbol{z}|/c)\,\mathrm{d}\boldsymbol{z} \\ &= -\frac{\omega_0^2}{16\pi^2} \iiint_{|\boldsymbol{x}-\boldsymbol{z}| \leqslant ct} \frac{\hat{\nu}(\boldsymbol{z})}{|\boldsymbol{x} - \boldsymbol{z}|^2} A(t - 2|\boldsymbol{x} - \boldsymbol{z}|/c)\,\mathrm{e}^{\mathrm{i}\omega_0(t - 2|\boldsymbol{x}-\boldsymbol{z}|/c)}\,\mathrm{d}\boldsymbol{z}, \end{aligned} \tag{10}$$

where

$$\hat{\nu}(\boldsymbol{z}) \stackrel{\mathrm{def}}{=} \nu(\boldsymbol{z}) + \mathrm{i}\frac{4\pi\sigma(\boldsymbol{z})}{\omega_0 c^2}. \tag{11}$$

[1] Actual SAR antennas have a special structure that enables narrowly directed radiation patterns [4].

According to (10), the scattered field $E^{(sc)}$ can be interpreted as the result of application of a Fourier integral operator (FIO), see, e.g., [4, 9–11], to the complex reflectivity function $\hat{\nu}(z)$ of (11) that combines the variation of the propagation speed c, see (7), and the variation of the conductivity σ. This FIO can be approximately inverted by applying a matched filter to $E^{(sc)}$ and accumulating the information due to multiple interrogating pulses (8) emitted from and received by the antenna at different locations along its trajectory. This is the procedure of SAR signal processing [4, 8, 12]; it allows one to reconstruct $\hat{\nu}(z)$, i.e. to obtain the image. Mathematically, this procedure is similar to the application of the adjoint operator, which would have coincided with the true inverse of FIO (10) if the latter were a genuine Fourier transform.

In general, $\hat{\nu}(z)$ is a function of three variables, because $z \in \mathbb{R}^3$. As, however, the synthetic antenna is aligned with the flight trajectory or orbit, which is one dimensional, the conventional SAR data collection algorithm (in the case of a monostatic non-interferometric sensor) can generate only two-dimensional datasets; see [4]. At the same time, the primary task of all practical SAR systems is imaging of the surface of the Earth from an aircraft or from satellites. The introduction of the Earth's surface as the geometric location (i.e. locus) of all the targets naturally eliminates the third coordinate (i.e. fixes the altitude) and hence makes the dimension of the dataset equal to that of the desired image. Mathematically, this corresponds to considering the reflectivity function (11) in the form

$$\hat{\nu}(z) \equiv \hat{\nu}(z_1, z_2, z_3) = \hat{\nu}(z_1, z_2)\delta(z_3), \tag{12}$$

i.e. in the form of a single layer on the surface, where z_1 and z_2 are the two horizontal coordinates and z_3 is the vertical coordinate [8]. The resulting image then reconstructs $\hat{\nu}(z_1, z_2)$, i.e. yields the complex reflectivity function (11) on the surface of the Earth as a function of the two horizontal coordinates.

In real applications, however, disregarding the polarization may not be appropriate, as the field is always polarized, and its polarization may change due to the interaction with the target[2]. Even in the simplest possible scenario, when a linearly polarized incident wave impinges on a plane interface between the vacuum and an isotropic target material, the polarization angle, generally speaking, tilts. A more sophisticated target material gives rise to a broader variety of possible changes in the polarization of the scattered field; see section 2. Mathematically, scattering off interfaces corresponds to a non-smooth permittivity $\boldsymbol{\varepsilon}(\boldsymbol{x})$ and/or conductivity $\boldsymbol{\sigma}(\boldsymbol{x})$, when the regions of their regular behavior (the vacuum and the target) are separated by a surface, at which these quantities (tensors) undergo jumps. Special boundary conditions are required at this surface for a proper description of the scattering mechanism.

The methodology of SAR imaging that takes into account the polarization of interrogating waves is known as the polarimetric SAR; see [13, 14]. As the antenna is typically far away from the target, by the time the incident pulse reaches the target it can be sufficiently accurately approximated by a transverse plane wave. Likewise, the scattered field can be effectively thought of as a transverse plane wave by the time it reaches the antenna. Therefore, even though the field vectors in $\mathbb{R}^3$ are three dimensional, it is sufficient to consider only their two transverse components if the third coordinate axis is chosen parallel to the direction of propagation. Accordingly, there are two independent linear polarizations for either the incident or scattered wave.

The theory of polarimetric SAR imaging is different from the scalar theory in that it exploits a completely phenomenological framework; the polarimetric SAR literature has been dominated by the phenomenological approach since the dissertation by Huynen [15]. Namely, the vector of the incident electric field that has two (transverse) components and the vector of

[2] It may also change due to the propagation in a chiral medium, e.g., the magnetized ionosphere.

the scattered electric field that also has two components are considered related by means of a formal 2×2 matrix $\mathcal{S}$:

$$\boldsymbol{E}^{(\mathrm{sc})} = \mathcal{S}\boldsymbol{E}^{(\mathrm{inc})}, \tag{13}$$

called the Sinclair scattering matrix. The entries of the scattering matrix $\mathcal{S}$ are usually not related to any physical characteristics of the target; they are rather introduced as the coefficients of the transformation between $\boldsymbol{E}^{(\mathrm{inc})}$ and $\boldsymbol{E}^{(\mathrm{sc})}$. This is precisely what the phenomenological nature of the approach of [15] means.

Note also that as the incident and scattered waves propagate in different directions, they will be represented in different coordinate systems in formula (13), and hence the scattering matrix $\mathcal{S}$ incorporates not only the transformation of the field per se, but also the change of the coordinates. Moreover, as both fields related by (13) are assumed transverse plane waves, they are attributed to different spatial locations—the target for the incident field and the receiving antenna for the scattered field. In the time domain, which is common for SAR applications [4], this would have also implied that the incident and scattered fields were evaluated at different moments in time.

Note that using formula (10), one can also obtain a scalar counterpart of relation (13). Consider a point scatterer of complex magnitude $\hat{\nu}$ located at z_0 so that $\hat{\nu}(z) = \hat{\nu}\delta(z - z_0)$. Then, instead of (10), we can write (with the help of (9))

$$E^{(\mathrm{sc})}(\boldsymbol{x}, t) \approx \underbrace{-\frac{\omega_0^2}{4\pi}\frac{\hat{\nu}}{|\boldsymbol{x} - z_0|}}_{S} E^{(\mathrm{inc})}(z_0, t - |\boldsymbol{x} - z_0|/c). \tag{14}$$

However, unlike the reflectivity function (11) that enters into (14) and (10), the entries of the scattering matrix $\mathcal{S}$ of (13) do not directly represent any physics-based scattering mechanism or material characteristics of the target; they are introduced just as the coefficients of a linear transformation. Subsequently, various target decomposition techniques (see section 4 and [14, chapters 4, 6, 7] for more details) attempt to attribute some physical properties of the target (e.g., its symmetry, convexity, etc) to certain combinations of the entries of the observed matrix $\mathcal{S}$.

For SAR applications, one often considers two basic cases of a linearly polarized incident field: horizontal polarization corresponds to the electric field vector normal to the plane of incidence, whereas vertical polarization corresponds to the electric field vector parallel to the plane of incidence. All other polarizations can be obtained as linear combinations of these two. Accordingly, the entries of the scattering matrix (that are also referred to as channels) are commonly denoted as

$$\mathcal{S} = \begin{bmatrix} S_{\mathrm{HH}} & S_{\mathrm{HV}} \\ S_{\mathrm{VH}} & S_{\mathrm{VV}} \end{bmatrix}, \tag{15}$$

where for each matrix entry, the first and second letter of the subscript denote the polarization of the scattered and incident field, respectively. In formula (15), S_{HH} and S_{VV} are the co-polarized channels, and S_{HV} and S_{VH} are the cross-polarized channels. Fully polarimetric SAR sensors produce four different images—one per channel[3].

In the frequency domain, the components of the electric field vector become complex, and instead of the retarded time, as in formula (14), the solution acquires the corresponding phase factor. The Sinclair matrix can then be represented as follows:

$$\mathcal{S} = \mathrm{e}^{\mathrm{i}\phi_0}\begin{bmatrix} |S_{\mathrm{HH}}| & |S_{\mathrm{HV}}|\,\mathrm{e}^{\mathrm{i}\phi_{\mathrm{HV}}} \\ |S_{\mathrm{VH}}|\,\mathrm{e}^{\mathrm{i}\phi_{\mathrm{VH}}} & |S_{\mathrm{VV}}|\,\mathrm{e}^{\mathrm{i}\phi_{\mathrm{VV}}} \end{bmatrix}, \tag{16a}$$

[3] In some inversion algorithms, the processing is not done channel by channel, but rather couples the channels, which may provide additional benefits; see, e.g., [16].

where ϕ_0 is the common phase (also called the absolute phase) that basically yields the distance (or time) that the scattered wave travels between the target and the receiving antenna, and ϕ_{HV}, ϕ_{VH} and ϕ_{VV} are the relative phases. In particular, ϕ_{VV} is called the co-polarized phase difference (CPD). The absolute phase ϕ_0 is the principal quantity of interest in the case of the SAR imaging by means of a scalar field; see, e.g., [8]. In that case, ϕ_0 helps determine the distance to the target, whereas the differences between the absolute phases of successive pulses provide the mechanism of azimuthal resolution.

In the vector case, representation (16*a*) clearly shows that the complex-valued Sinclair scattering matrix offers a total of seven additional degrees of freedom—four amplitudes and three relative phases—on top of the scalar case. Consequently, eight independent quantities (1+7) associated with every location yield as much information as one can obtain from a polarimetric SAR image (i.e. four complex-valued images, one per channel) regardless of what the actual target is.

We should also mention that extracting the common phase ϕ_0 the way it is done in formula (16*a*) removes a certain degree of arbitrariness that otherwise exists in the definitions. Indeed, the scattering mechanism at the target can be such that every polarization undergoes a phase shift upon reflection; see section 2. In this case, instead of (16*a*), we would have

$$\mathcal{S} = \mathrm{e}^{\mathrm{i}\tilde{\phi}_0}\begin{bmatrix} |S_{\mathrm{HH}}|\,\mathrm{e}^{\mathrm{i}\tilde{\phi}_{\mathrm{HH}}} & |S_{\mathrm{HV}}|\,\mathrm{e}^{\mathrm{i}\tilde{\phi}_{\mathrm{HV}}} \\ |S_{\mathrm{VH}}|\,\mathrm{e}^{\mathrm{i}\tilde{\phi}_{\mathrm{VH}}} & |S_{\mathrm{VV}}|\,\mathrm{e}^{\mathrm{i}\tilde{\phi}_{\mathrm{VV}}} \end{bmatrix} \stackrel{\mathrm{def}}{=} \mathrm{e}^{\mathrm{i}\tilde{\phi}_0}\tilde{\mathcal{S}}, \tag{16b}$$

where the entries of the matrix represent the actual complex reflection coefficients, and $\tilde{\phi}_0$ accounts for the travel distance. The relation between the phases in (16*a*) and (16*b*) is obvious: $\phi_0 = \tilde{\phi}_0 + \tilde{\phi}_{\mathrm{HH}}$, but having only the overall matrix $\mathcal{S}$ as an observable, one cannot tell unambiguously how to split ϕ_0 into $\tilde{\phi}_0$ and $\tilde{\phi}_{\mathrm{HH}}$. Therefore, it is common in the literature to adopt normalization (16*a*) that keeps the HH entry of the matrix real.

Modern practical applications of radar polarimetry employ different empirical and semi-empirical criteria that rely on the entries of the scattering matrix $\mathcal{S}$. Examples include a CPD-based study of oil spills [17], an algorithm for reconstructing the ocean surface slopes that utilizes all four channels [18], several soil moisture retrieval algorithms analyzed in [19] and vegetation classification technique that uses multi-frequency polarimetric data [20]. Additional references can be found in [14].

1.4. Objectives of the paper

Our primary objective is to build a material-based linearized scattering model for the case of vector propagation. In other words, using the first Born approximation, we would like to relate the entries of the scattering matrix $\mathcal{S}$ to the material properties of the target (its permittivity and conductivity), similarly to how one defines the ground reflectivity function in the scalar case; see formulae (7), (11) and (14).

Note that in the framework of the first Born approximation, one can formulate both a direct and an inverse scattering problem. The direct problem consists in obtaining the scattered field $\boldsymbol{E}^{(\mathrm{sc})}$, given the incident field $\boldsymbol{E}^{(\mathrm{inc})}$ and the material parameters $\boldsymbol{\varepsilon}$ and $\boldsymbol{\sigma}$, and assuming that the scattering is weak (see section 1.2). Of our primary interest is the corresponding linearized inverse scattering problem, which consists in defining channels (15) as functions of the material parameters, $S_{\mathrm{HH}} = S_{\mathrm{HH}}(\boldsymbol{\varepsilon}, \boldsymbol{\sigma})$, $S_{\mathrm{VV}} = S_{\mathrm{VV}}(\boldsymbol{\varepsilon}, \boldsymbol{\sigma})$, $S_{\mathrm{HV}} = S_{\mathrm{HV}}(\boldsymbol{\varepsilon}, \boldsymbol{\sigma})$ and $S_{\mathrm{VH}} = S_{\mathrm{VH}}(\boldsymbol{\varepsilon}, \boldsymbol{\sigma})$, so that $\boldsymbol{\varepsilon}$ and $\boldsymbol{\sigma}$ can subsequently be reconstructed given the fields $\boldsymbol{E}^{(\mathrm{inc})}$ and $\boldsymbol{E}^{(\mathrm{sc})}$ in formula (13), and again assuming that the scattering is weak.

The desired linearized scattering model shall be minimally complex in terms of the structure of the tensors $\boldsymbol{\varepsilon}$ and $\boldsymbol{\sigma}$. This means that it should not aim at more than recovering

the four complex reflection coefficients contained in the matrix $\tilde{\mathcal{S}}$ of (16*b*), which is a total of eight degrees of freedom, because what the polarimetric SAR methodology is capable of detecting is even one degree of freedom less; see formula (16*a*).

Availability of such a model may help develop the radar ambiguity theory[4] for the polarimetric case similarly to how it is done in the scalar case; see [8]. Besides, it may prove useful for the material identification SAR (miSAR) applications.

The application of the first Born approximation in the vector case is similar to that in the scalar case (discussed in section 1.2). Replacing the total electric field $\boldsymbol{E}$ by the incident field $\boldsymbol{E}^{(\mathrm{inc})}$ on the right-hand side of equation (A.4) and taking into account the Gauss laws $\nabla \cdot \boldsymbol{D} = 0$ and $\nabla \cdot \boldsymbol{E}^{(\mathrm{inc})} = 0$, we obtain

$$\frac{1}{c^2}\frac{\partial^2 \boldsymbol{E}^{(\mathrm{sc})}}{\partial t^2} - \Delta \boldsymbol{E}^{(\mathrm{sc})} = -\frac{\boldsymbol{\varepsilon} - \mathcal{I}}{c^2} \cdot \frac{\partial^2 \boldsymbol{E}^{(\mathrm{inc})}}{\partial t^2} - \frac{4\pi\boldsymbol{\sigma}}{c^2} \cdot \frac{\partial \boldsymbol{E}^{(\mathrm{inc})}}{\partial t}. \tag{17}$$

The main difference between this equation and its counterpart for the isotropic case, equation (6), is that the material characteristics in equation (17) are tensors rather than scalars. This implies that generally speaking, the vector equation (17) cannot be decoupled into the independent scalar equations for the individual field components. Moreover, studying the scattering of electromagnetic waves off interfaces requires special boundary conditions in addition to the governing equations themselves. Those boundary conditions play a key role in the construction of the first Born approximation for the case of vector fields; see section 2.

In section 2 of the paper, we carefully develop and analyze the first Born approximation as it applies to scattering off a hierarchy of target materials. Starting with the simplest case of an isotropic dielectric, we gradually increase the complexity of the material by allowing for the anisotropy of $\boldsymbol{\varepsilon}$ and including the weak conductivity $\boldsymbol{\sigma}$ (anisotropic as well) so that finally we reach the same number of the degrees of freedom as in (16*a*). The resulting material is a uniaxial crystal (i.e. a birefringent medium) with the conductivity tensor that is also uniaxial, and with both axes allowed to have arbitrary directions with respect to the incidence plane and with respect to one another. We prove that the scattered field in vacuum obtained in this linearized framework approximates the true reflected field that one can obtain with no use of the Born approximation. We also obtain a necessary and sufficient condition for the existence of a solution to the foregoing linearized inverse scattering problem. Under this condition, the scattering matrix (16*a*) can be obtained by appropriately choosing the permittivities, conductivities and angles that define the material and the orientation of its optical axis with respect to the plane of incidence.

The second objective of this paper is related to the first one. Namely, in the linearized framework that we have adopted for describing the scattering, a formal mathematical justification is needed for the possibility of taking the ground reflectivity function in the form of a single layer on the surface; see formula (12).

As of yet, the transition from the entire half-space occupied by the target material to the target material concentrated only on the surface has been motivated by the mere convenience of having the third coordinate removed from the radar dataset[5]; see the discussion around equation (12). This, however, is not a rigorous argument. One rather needs to prove that the linearized scattering off a material half-space can be equivalently reformulated as the linearized scattering off a layer of monopoles at its surface only.

[4] The approach to the theoretical assessment of the radar performance based on the analysis of the radar ambiguity function; see, e.g., [4, chapters 5 and 11].

[5] It is also supported by physical reasoning in the literature. For the microwave carrier frequencies ω_0, the penetration depth of the radar signals into the ground is very small, and all the reflections must be those off the surface. However, the first Born approximation may lead to a certain inconsistency for the ground reflectivity function in the form (12). Indeed, the single layer radiates in both directions, vacuum and material, which means that the scattered field actually penetrates into the ground.

In other words, we arrive at the following inverse source [21] problem: for the linearized scattering off a half-space, find an equivalent surface reflectivity function of type (12) that would yield the same scattered field in the vacuum region. In section 3, we solve this inverse source problem and show that in the scalar case, the resulting 'density' $\hat{\nu}(z_1, z_2)$ indeed appears proportional to the target reflectivity function (11) on the surface. Moreover, we formulate and solve a similar inverse source problem in the vector case as well. With the polarization taken into account, the scattered field in the vacuum region can also be represented as a single-layer surface potential with tensor densities proportional to the jumps of the material characteristics at the interface. These topics are addressed in section 3, whereas in section 4, we discuss the relation between our analysis and polarimetric target decomposition.

The main notation that will be used hereafter is explained in table 1.

2. Hierarchy of scattering models

2.1. Roadmap

In section 2, we present a detailed derivation of the first Born approximation for the scattering of a linearly polarized electromagnetic wave off a material half-space. We consider several types of materials: a perfect isotropic dielectric, a perfect birefringent (uniaxial) dielectric and lossy isotropic and birefringent dielectrics. In each case, our first goal is to determine the number of degrees of freedom associated with a given material in the linearized direct scattering problem. This number is determined by the functional dependence of the reflection coefficients on the material parameters.

In section 2.3, the scattering coefficients are derived for the isotropic case. First, the Maxwell equations are transformed to the frequency domain, and the dependence of their solution on the tangential variables is factored out using the uniformity of the formulation along the interface. Then, the equations are linearized and reduced to a second-order ordinary differential equation (ODE) that governs the propagation of the scattered field in the direction normal to the interface. This equation is supplemented by the radiation conditions at infinity and the matching conditions at the interface. It turns out that the key difference between the horizontal and vertical polarizations is precisely in the interface conditions. For the horizontal polarization, those conditions reduce to the continuity of the solution itself and its first derivative across the interface. For the vertical polarization, the condition for the first derivative becomes inhomogeneous, and this derivative undergoes a jump across the interface. Accordingly, the reflection coefficients are different for two polarizations, while the dielectric permittivity provides a single degree of freedom for this setting.

We note that the first Born approximation in the scalar (i.e. isotropic) case has been extensively studied in the literature, and also used in the context of SAR applications. The reason we include its detailed analysis in this paper is twofold. On one hand, it allows us to build the framework and introduce the solution methodology that subsequently applies to the cases with anisotropy and/or Ohmic losses. On the other hand, in its own right it helps us emphasize a very important distinction between the horizontal and vertical incident polarizations. In the case of a horizontal polarization, the linearized interface condition is homogeneous, and this is precisely the case that has received most of the attention in the literature; see, e.g., [5]. For the vertical polarization though, the linearized interface condition becomes inhomogeneous and accordingly, the solution given by the first Born approximation is different even though the linearized governing equation is the same as in the case of a horizontal polarization.

In the lossless anisotropic case (section 2.4), the polarizations are no longer independent, and Maxwell's equations reduce to a system of two coupled ODEs that govern the components

Table 1. Key notation and its relations to be used hereafter.

Parameter name	Notation	Relations	Reference
Dielectric tensor and its reciprocal	$\boldsymbol{\varepsilon}$, $\boldsymbol{\eta}$	$\boldsymbol{D} = \boldsymbol{\varepsilon} \cdot \boldsymbol{E}$; $\boldsymbol{\varepsilon} \cdot \boldsymbol{\eta} = \mathcal{I}$	(18), (51)
Isotropic permittivity (or dielectric constant)	ε, $\varepsilon(z)$	$\varepsilon(z) = 1 + \theta(z)(\varepsilon - 1)$	(23)
Geometry and parameters of the uniaxial dielectric tensor	$\varepsilon_\perp$, $\varepsilon_\parallel$, $\Delta\varepsilon$, α, β, γ	$\Delta\varepsilon = \varepsilon_\parallel - \varepsilon_\perp$, $\alpha^2 + \beta^2 + \gamma^2 = 1$	(48)–(50)
Entries of the reciprocal dielectric tensor	η_{ij},$i, j = x, y, z$	$\eta_{ii} = 1/\varepsilon_{ii}$; $\eta_{ij} = -\varepsilon_{ij}$ for $i \neq j$	(52)
Conductivity tensor	$\boldsymbol{\sigma}$	$\boldsymbol{j} = \boldsymbol{\sigma} \cdot \boldsymbol{E}$	(3)
Isotropic conductivity	σ	$\boldsymbol{j} = \sigma \boldsymbol{E}$	(79)
Geometry and parameters of the uniaxial conductivity tensor	$\sigma_\perp$, $\sigma_\parallel$, $\Delta\sigma$, α_σ, β_σ, γ_σ	$\Delta\sigma = \sigma_\parallel - \sigma_\perp$, $\alpha_\sigma^2 + \beta_\sigma^2 + \gamma_\sigma^2 = 1$	section 2.5.1
Modified permittivity in the frequency domain	$\tilde{\boldsymbol{\varepsilon}}$	$\tilde{\boldsymbol{\varepsilon}} = \boldsymbol{\varepsilon} + \mathrm{i}\frac{4\pi}{\omega}\boldsymbol{\sigma}$	(81)
Small parameter for the first Born approximation	$\varkappa$	$\|\boldsymbol{\varepsilon} - \mathcal{I}\| \sim \varkappa$, $\|\boldsymbol{\sigma}\| \sim \varkappa\omega$, $\|u^{(\mathrm{sc})}\| \sim \varkappa\|u_0\|$	(22), (25*c*)
Differential operator describing scattering, right-hand-side parameter	$\hat{L}$, r	$\hat{L} = \dfrac{\mathrm{d}^2/\mathrm{d}z^2 + q^2}{q^2}$	(28)
Electromagnetic field, its components and amplitudes	U; $u^{(\mathrm{inc})}$, $u^{(\mathrm{sc})}$; u_0, $u(z)$	$U = u^{(\mathrm{inc})} + u^{(\mathrm{sc})}$, $u^{(\mathrm{inc})} = u_0\,\mathrm{e}^{\mathrm{i}(qz+Kx)}$, $\|u^{(\mathrm{sc})}\| \sim \varkappa\|u_0\|$	(24)–(27)
Undetermined coefficients for a solution in two domains	A, B, C	$u^{(\mathrm{sc})}(z) = (Az + B)u_0\,\mathrm{e}^{\mathrm{i}qz}$ for $z > 0$; $u^{(\mathrm{sc})}(z) = Cu_0\,\mathrm{e}^{-\mathrm{i}qz}$ for $z < 0$	(33)
Free space and material sides of the interface at $z = 0$	(F), (M)	$(F) \equiv (z = -0)$ $(M) \equiv (z = +0)$	(20), figure 1
Boundary condition parameter	R	$\frac{\mathrm{d}u}{\mathrm{d}z}\big\|_{(M)} = \frac{\mathrm{d}u}{\mathrm{d}z}\big\|_{(F)} + Ru_0$	(34), (35)
Wave vector and its components	k. K, q	$k^2 = K^2 + q^2$; $K = k\sin\theta_i$	(21), (41), figure 1
Polarization ratio	Q	$S_{\mathrm{VV}} = S_{\mathrm{HH}}Q$,	(45), (74), (75), (77), (83), figure 2

of the electric and magnetic field normal to the plane of incidence. For this system, the first Born approximation appears very convenient to implement in two stages: first the equations are uncoupled and then the resulting individual equations are linearized. The end result depends on the polarization of the incident wave. In each case (vertical or horizontal incident polarization), one of the uncoupled equations describes the co-polarized scattering and the other describes the cross-polarized scattering. The form of the resulting equations and interface conditions turns out to be similar to the isotropic case, although the actual expressions for the reflection coefficients are not the same and contain additional degrees of freedom.

In the case of a lossy material (section 2.5), we show that the presence of a weak conductivity is equivalent to having a small imaginary part in the overall complex permittivity, which, in turn, makes the small parameter of the first Born approximation complex. This

Table 2. Overview of scattering models and their properties: material parameters, non-zero reflection coefficients and the maximum number of degrees of freedom. The wavy underline in the third column means that the values may be complex.

Model of scatterer	Independent material parameters	Non-zero reflection coefficients	Max. number of d.o.f.	Section #
Perfect isotropic dielectric	ε	HH, VV	1	2.3
Lossy isotropic dielectric	ε, σ	HH, VV	1	2.5.2
Perfect uniaxial dielectric, interface in the basal plane	$\varepsilon_\perp, \varepsilon_\parallel$	HH, VV	2	2.4.5
Lossy uniaxial dielectric with spherical conductivity tensor, interface in the basal plane	$\varepsilon_\perp, \varepsilon_\parallel, \sigma$	HH, VV	3	2.5.3
Perfect uniaxial dielectric, the arbitrary direction of optical axis	$\varepsilon_\perp, \varepsilon_\parallel, \alpha, \gamma$	HH, VV, HV, VH	4	2.4.7
Lossy uniaxial dielectric, the arbitrary direction of optical axis	$\varepsilon_\perp, \varepsilon_\parallel, \alpha, \gamma,$ $\sigma_\perp, \sigma_\parallel, \alpha_\sigma, \gamma_\sigma$	HH, VV, HV, VH	8	2.5.4

observation significantly simplifies the treatment of the lossy materials. In particular, the functional representation of the imaginary part of the scattering matrix turns out to be the same as that of the real part. Hence, the anisotropic conductivity yields the same number of degrees of freedom as does the anisotropic permittivity.

In table 2, we provide the number of degrees of freedom and list the independent material parameters for each of the cases we have considered.

Having identified the degrees of freedom that characterize every material included into our analysis, we move on toward addressing the next goal of this section, which is to solve the corresponding linearized inverse scattering problem. Specifically, we would like to see whether a given scattering matrix can be obtained by adjusting the available degrees of freedom, i.e. by appropriately choosing the characteristics of the target material. In theorem 1, we furnish a necessary and sufficient condition for the solvability of this inverse problem in the case of a lossless birefringent material, and in corollary 1, we extend this result to the case of a lossy anisotropic material.

2.2. General formulation

We consider the scattering of a monochromatic plane wave off a material half-space with permittivity tensor $\boldsymbol{\varepsilon}$ and conductivity tensor $\boldsymbol{\sigma}$. Since all the fields depend on time as $\mathrm{e}^{-\mathrm{i}\omega t}$, where ω is the frequency, we conduct the analysis in the frequency domain. For transverse electromagnetic waves with no extraneous currents[6], the unsteady equations of the system (1) with equation (3) taken into account reduce to

$$\nabla \times \boldsymbol{E} = \mathrm{i}k\boldsymbol{H} \quad \text{and} \quad \nabla \times \boldsymbol{H} = -\mathrm{i}k\boldsymbol{D} + \frac{4\pi}{c}\boldsymbol{\sigma} \cdot \boldsymbol{E}, \tag{18}$$

where $k = \omega/c$. Equation (2) and the Gauss laws of electricity and magnetism (steady-state equations in (1)) keep their form in the frequency domain.

Denote $\boldsymbol{x} = (x, y, z) \in \mathbb{R}^3$ and assume that the half-space $z < 0$ is occupied by vacuum, whereas the half-space $z > 0$ is filled with the material. The plane of incidence is defined as to contain the wave vector of the incident wave and the normal to the interface $z = 0$; with no loss of generality, we take it as the (x, z) plane (see figure 1). The problem is essentially two

[6] The excitation in the problem will be provided by incident plane waves.

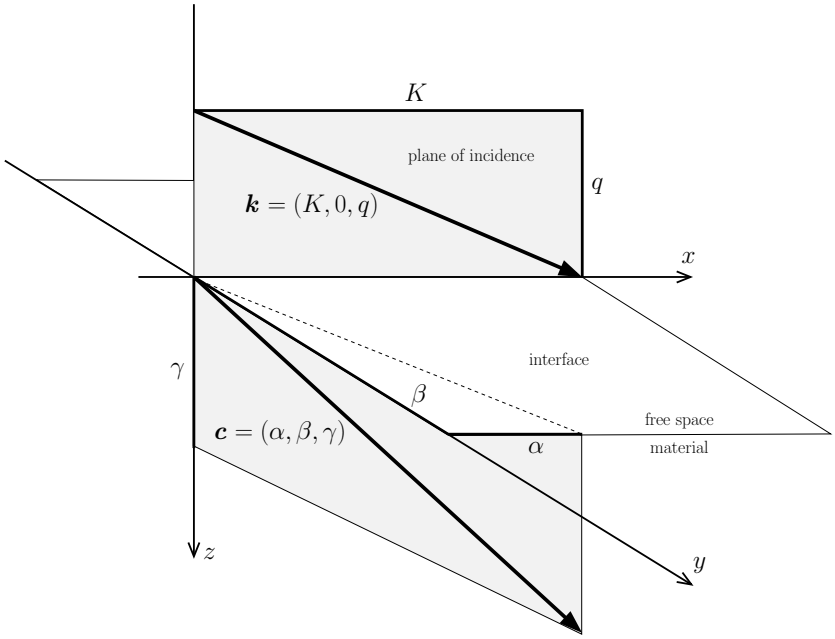

Figure 1. Schematic for the scattering problem off an anisotropic half-space. The vector $\boldsymbol{k} = (K, 0, q)$ is the incident wave vector, see formula (21). The vector $\boldsymbol{c} = (\alpha, \beta, \gamma)$ is a unit vector along the optical axis (see section 2.4). Note that α, β and γ denote the direction cosines rather than the actual angles.

dimensional, as the wave vectors of the incident, reflected and transmitted waves all belong to the plane of incidence. Hence, the electromagnetic fields do not depend on the y coordinate (although the vectors may have y components).

Then, the system (18) takes the form

$$\begin{aligned} -\frac{\partial E_y}{\partial z} &= \mathrm{i}kH_x, & -\frac{\partial H_y}{\partial z} &= -\mathrm{i}k\tilde{D}_x, \\ \frac{\partial E_x}{\partial z} - \frac{\partial E_z}{\partial x} &= \mathrm{i}kH_y, & \frac{\partial H_x}{\partial z} - \frac{\partial H_z}{\partial x} &= -\mathrm{i}k\tilde{D}_y, \\ \frac{\partial E_y}{\partial x} &= \mathrm{i}kH_z, & \frac{\partial H_y}{\partial x} &= -\mathrm{i}k\tilde{D}_z, \end{aligned} \tag{19}$$

where $\tilde{D}_x$, $\tilde{D}_y$ and $\tilde{D}_z$ are the components of the vector $\tilde{\boldsymbol{D}} = \boldsymbol{\varepsilon} \cdot \boldsymbol{E} + (4\pi\mathrm{i}/\omega)\boldsymbol{\sigma} \cdot \boldsymbol{E}$. In the free space (vacuum), we have $\boldsymbol{\varepsilon} = \mathcal{I}$ and $\boldsymbol{\sigma} = \boldsymbol{0}$.

At the interface $z = 0$, the following boundary conditions are imposed on the tangential components of the electric and magnetic field [2, 22]:

$$E_x|_{(F)} = E_x|_{(M)}, \quad E_y|_{(F)} = E_y|_{(M)}, \tag{20a}$$

$$H_x|_{(F)} = H_x|_{(M)}, \quad H_y|_{(F)} = H_y|_{(M)}. \tag{20b}$$

The subscripts (F) and (M) in formulae (20) denote the free space ($z = -0$) and material ($z = +0$) side of the interface, respectively.

The incident field in formulae (5) is chosen as a plane wave:

$$(\boldsymbol{E}^{(\mathrm{inc})}, \boldsymbol{H}^{(\mathrm{inc})}) = \left(\boldsymbol{E}_0^{(\mathrm{inc})}, \boldsymbol{H}_0^{(\mathrm{inc})}\right) \mathrm{e}^{\mathrm{i}(qz+Kx)}, \tag{21}$$

where K is the common horizontal wavenumber for all plane waves in the problem, and

$$q = (k^2 - K^2)^{1/2}$$

is the vertical component of the incident wave vector (see [2, 22, 23]).

In addition to the interface conditions (20) for the total field, the scattered field $(\boldsymbol{E}^{(\mathrm{sc})}, \boldsymbol{H}^{(\mathrm{sc})})$ should also satisfy the radiation conditions as $z \to \pm\infty$ (see formulae (29)).

In the textbook approach to problem (19)–(20) (see, e.g., [3, 2]), the incident field (21) is restricted to the free space, while the system (19) is solved with respect to the scattered field, and its solutions are found separately for the vacuum and material half-spaces. These solutions, called the reflected and transmitted fields, respectively, are combined with the incident field, and then matched at the interface using boundary conditions (20). A comprehensive account of this approach can be found, e.g., in [22]. For the particular case of a perfect isotropic dielectric, the amplitude and direction of the reflected and transmitted fields are given by the classic Fresnel's equations and Snell's law; these expressions (see, e.g., [2, 3]) are valid for the arbitrary values of ε. Besides, various simplifications can be considered depending on the specific structure of $\boldsymbol{\varepsilon}$ and $\boldsymbol{\sigma}$ [23].

As indicated in section 1.4, our goal is to analyze the linearized scattering case. Therefore, in the material domain $z > 0$, we assume that

$$\|\boldsymbol{\varepsilon} - \mathcal{I}\| \sim \varkappa \quad \text{and} \quad \|\boldsymbol{\sigma}\| \sim \varkappa\omega, \tag{22}$$

where $\varkappa$ is a small parameter, so that the scattering is weak. To study the existence of a solution to the resulting inverse scattering problem, we will use the first Born approximation to obtain a series of direct scattering solutions for a hierarchy of settings, starting from the simplest case, i.e. that of a perfect isotropic dielectric. The Fresnel and other exact solutions, linearized according to (22), will be used for the validation of the solutions obtained with the help of the first Born approximation.

2.3. The first Born approximation for a perfect isotropic dielectric

2.3.1. Governing equations. Assume that in the material, the dielectric tensor is spherical, which means that the permittivity is scalar, and that the conductivity is zero. Since $\boldsymbol{\sigma} = \mathbf{0}$, the components of the vector $\tilde{\boldsymbol{D}}$ in (19) can be replaced by those of $\boldsymbol{D}$. Since $\boldsymbol{\varepsilon} = \varepsilon(z)\mathcal{I}$ in the entire space, the vectors $\boldsymbol{D}$ and $\boldsymbol{E}$ are proportional, i.e.

$$D_i(x, z) = \varepsilon(z)E_i(x, z) \quad \text{for} \quad i = x, y, z,$$

where

$$\varepsilon(z) = 1 + \theta(z)(\varepsilon - 1), \tag{23}$$

$\theta(z)$ is a unit step function and $\varepsilon > 1$ is the permittivity in the material domain $z > 0$ (see [2, 3]). In this case, the equations for the variables E_x, E_z, H_y and for H_x, H_z, E_y in the system (19) are decoupled. This means that the system (19) admits a solution with $E_x = E_z = H_y = 0$, which is called horizontal polarization, and another solution with $H_x = H_z = E_y = 0$, called vertical polarization. Each of these solutions is governed by the scalar Helmholtz equation

$$\frac{\partial^2 U}{\partial x^2} + \frac{\partial^2 U}{\partial z^2} + \varepsilon(z)k^2 U = 0, \tag{24}$$

where $U(x, z)$ represents any nonzero Cartesian component of $\boldsymbol{E}$ or $\boldsymbol{H}$.

To build the first Born approximation for the scattering of a plane incident wave in either of the two basic polarizations defined above, we represent the total field U in (24) as a sum of the incident and scattered fields as in (5):

$$U = u^{(\mathrm{inc})} + u^{(\mathrm{sc})}, \tag{25a}$$

take the incident field in the form (21)

$$u^{(\mathrm{inc})} = u_0\, \mathrm{e}^{\mathrm{i}(qz+Kx)} \tag{25b}$$

and assume that

$$|u^{(\mathrm{sc})}| \sim \varkappa |u_0|, \tag{25c}$$

where the small parameter $\varkappa$ is introduced in (22). In doing so, both the incident and scattered components of the field occupy the entire space. Substituting equality (25*a*) into (24) and taking into account that $u^{(\mathrm{inc})}$ satisfies the same equation (24) but with $\varepsilon = 1$, we arrive at the equation for $u^{(\mathrm{sc})}$:

$$\frac{\partial^2 u^{(\mathrm{sc})}}{\partial x^2} + \frac{\partial^2 u^{(\mathrm{sc})}}{\partial z^2} + k^2 u^{(\mathrm{sc})} = -(\varepsilon(z) - 1)k^2 (u^{(\mathrm{inc})} + u^{(\mathrm{sc})}). \tag{26}$$

The first Born approximation consists in disregarding the second-order term $(\varepsilon - 1)u^{(\mathrm{sc})}$, see formulae (22) and (25*c*), on the right-hand side of equation (26). Moreover, as everything in our formulation is uniform along the plane (x, y), see figure 1, the dependence of the solution on x and y must be the same in the entire space (see [2, chapter X]). This, in particular, implies that the horizontal component of the wave vector is the same for both the incident field (21), (25*b*) and the scattered field, so that we can take

$$u^{(\mathrm{sc})} = u(z)\, \mathrm{e}^{\mathrm{i}Kx}. \tag{27}$$

Equation (27) helps us reduce (26) to the following equation for $u(z)$:

$$\frac{1}{u_0}\hat{L}u = g(z) \equiv -r\theta(z)\, \mathrm{e}^{\mathrm{i}qz}, \quad \hat{L} \stackrel{\mathrm{def}}{=} \frac{1}{q^2}\frac{\mathrm{d}^2}{\mathrm{d}z^2} + 1, \tag{28}$$

where $r = (\varepsilon - 1)k^2/q^2$. Note that the incident field satisfies the equation $\hat{L}u^{(\mathrm{inc})} = 0$. The solution $u(z)$ of equation (28) should also satisfy the radiation conditions at infinity:

$$\frac{1}{\mathrm{i}q}\frac{\mathrm{d}u}{\mathrm{d}z} - u = 0 \quad \text{as} \quad z \to \infty \qquad \text{and} \qquad \frac{1}{\mathrm{i}q}\frac{\mathrm{d}u}{\mathrm{d}z} + u = 0 \quad \text{as} \quad z \to -\infty. \tag{29}$$

The overall solution to equation (28) will be obtained as the sum of the general solution to the corresponding homogeneous equation and a particular solution to the inhomogeneous equation (28). For the general solution to the homogeneous equation $\hat{L}u = 0$ subject to the radiation conditions (29), we can write

$$u^{(\mathrm{h})}(z) = \begin{cases} Bu_0\, \mathrm{e}^{\mathrm{i}qz}, & z > 0, \\ Cu_0\, \mathrm{e}^{-\mathrm{i}qz}, & z < 0, \end{cases} \tag{30}$$

where B and C are constants. A particular solution to the inhomogeneous equation (28), which accounts for the resonance between $\hat{L}$ and $g(z)$ on the material domain $z > 0$, is given by

$$u^{(\mathrm{p})}(z) = \begin{cases} Au_0 z\, \mathrm{e}^{\mathrm{i}qz}, & z > 0, \\ 0, & z < 0, \end{cases} \tag{31}$$

where the value of A is obtained by the method of undetermined coefficients:

$$A = \frac{\mathrm{i}rq}{2}. \tag{32}$$

Combining (30) and (31), we obtain the overall scattering solution in the form

$$u^{(\mathrm{sc})}(z) = \begin{cases} (Az + B)u_0\, \mathrm{e}^{\mathrm{i}qz}, & z > 0 \quad \text{(material)}, \\ Cu_0\, \mathrm{e}^{-\mathrm{i}qz}, & z < 0 \quad \text{(vacuum)}, \end{cases} \tag{33}$$

where the constants B and C shall be determined with the help of the interface conditions (20). The constant C can be interpreted as the reflection coefficient.

In sections 2.3.2 and 2.3.3, we will show that whereas the governing differential equation (28) and the value of r on its right-hand side are the same for both polarizations, the interface conditions (20), as expressed via the single unknown function u, appear different for the horizontal and vertical polarizations. Specifically, in either case the interface conditions can be written as

$$u|_{(M)} = u|_{(F)}\,; \qquad \left.\frac{\mathrm{d}u}{\mathrm{d}z}\right|_{(M)} = \left.\frac{\mathrm{d}u}{\mathrm{d}z}\right|_{(F)} + Ru_0, \tag{34}$$

where the constant R depends on the polarization (it may be equal to zero). Accordingly, solution (33) also appears different for the horizontal and vertical polarizations. In particular, substituting (33) and (32) into (34), we can express the reflection coefficient C via the parameters r and R:

$$C = B = -\frac{r}{4} + \frac{R}{2\mathrm{i}q}, \tag{35}$$

which indicates that the reflection coefficient depends on the polarization via R.

Finally, let us note that equation (28) can also be solved by convolution with the fundamental solution (see, e.g., [5]). As we explain in section 3 though, the deficiency of this approach is precisely in that it offers no easy way of accounting for the different interface conditions (i.e. different values of R) that correspond to different polarizations.

2.3.2. Horizontal polarization. In this case, the unknown quantity in equation (24) is usually taken as $U = E_y$, with the other two nonzero field components being H_x and H_z. The first equation (19) then implies

$$H_x = \frac{\mathrm{i}}{k}\frac{\mathrm{d}E_y}{\mathrm{d}z}, \tag{36}$$

so that boundary conditions (20) reduce to

$$E_y|_{(F)} = E_y|_{(M)} \quad \text{and} \quad \left.\frac{\mathrm{d}E_y}{\mathrm{d}z}\right|_{(F)} = \left.\frac{\mathrm{d}E_y}{\mathrm{d}z}\right|_{(M)}. \tag{37}$$

Boundary conditions (37) imply the continuity of the total field (25*a*) and its first normal derivative at the interface. As the incident field (25*b*) and its derivative are continuous at $z = 0$, so are the scattered field $u^{(\mathrm{sc})} = E_y^{(\mathrm{sc})}$ and its first derivative with respect to z:

$$E_y^{(\mathrm{sc})}\big|_{(F)} = E_y^{(\mathrm{sc})}\big|_{(M)} \quad \text{and} \quad \left.\frac{\mathrm{d}E_y^{(\mathrm{sc})}}{\mathrm{d}z}\right|_{(F)} = \left.\frac{\mathrm{d}E_y^{(\mathrm{sc})}}{\mathrm{d}z}\right|_{(M)}. \tag{38}$$

Conditions (38) are used to determine the constants B and C in (33). A comparison of (38) to (34) shows that $R = 0$, so, according to (35), the co-polarized reflection coefficient for the horizontal polarization is given by[7]

$$S_{\mathrm{HH}} \overset{\mathrm{def}}{=} C = B = -\frac{r}{4} = -\frac{1}{4}\frac{k^2}{q^2}(\varepsilon - 1). \tag{39}$$

[7] Hereafter, we identify the reflection coefficients with the entries of the scattering matrix $\mathcal{S}$ of (15); see section 2.3.4.

At the same time, the Fresnel solution [3, chapter I] gives the following expression for the exact reflection coefficient in the case of horizontal polarization:

$$S_{\mathrm{HH}}^{(\mathrm{exact})} = -\frac{\sin(\theta_i - \theta_t)}{\sin(\theta_i + \theta_t)}, \tag{40}$$

where θ_i is the incidence angle and θ_t is the refraction angle (defined by Snell's law):

$$\sin\theta_i = \frac{K}{k}, \qquad \sin\theta_t = \frac{1}{\sqrt{\varepsilon}}\sin\theta_i. \tag{41}$$

Formulae (40) and (41) do not involve linearization and are valid for arbitrary values of ε.

A comparison of the linearized solution (33), (32) and (39) to the Fresnel solution (40), (41) shows the deficiency of the former: in the material, it has a component that grows linearly as z increases, which is not physical. In addition, expression (33) does not provide the correct wavenumber and propagation direction of the refracted wave, which restricts the validity of the first Born approximation inside the material to the area [6]:

$$|z| \leqslant z_0 \sim \frac{\pi}{|q - q^{(\mathrm{exact})}|} \approx \frac{2\pi q}{k^2|\varepsilon - 1|},$$

where $q^{(\mathrm{exact})}$ is the z-component of the refracted wavenumber obtained from Snell's law:

$$q^{(\mathrm{exact})} = \sqrt{\varepsilon}k\cos\theta_t = k\sqrt{\varepsilon - \sin^2\theta_i},$$

see the second equation in formula (41).

However, formulae (33) and (39) are useful in the vacuum region: the wavenumber and propagation direction of the scattered field in vacuum are correct, and one can also see that the reflection coefficient (39) given by the first Born approximation coincides with the linear term in the expansion of the exact reflection coefficient (40) in powers of $\varkappa = \varepsilon - 1$. Indeed, using equations (41) and taking into account that $\cos\theta_i = q/k$ and also

$$\varepsilon\cos^2\theta_t = \varepsilon - (1 - \cos^2\theta_i) = \cos^2\theta_i\left(1 + \varkappa\frac{k^2}{q^2}\right),$$

we can transform expression (40) as follows:

$$\begin{aligned} S_{\mathrm{HH}}^{(\mathrm{exact})} &= \frac{\frac{1}{\sqrt{\varepsilon}}\sin\theta_i\cos\theta_i - \frac{1}{\sqrt{\varepsilon}}\cos\theta_i\sin\theta_i(1 + \varkappa k^2/q^2)^{1/2}}{\frac{1}{\sqrt{\varepsilon}}\sin\theta_i\cos\theta_i + \frac{1}{\sqrt{\varepsilon}}\cos\theta_i\sin\theta_i(1 + \varkappa k^2/q^2)^{1/2}} \\ &= \frac{1 - (1 + \varkappa k^2/q^2)^{1/2}}{1 + (1 + \varkappa k^2/q^2)^{1/2}} = -\frac{1}{4}\frac{k^2}{q^2}\varkappa + \mathcal{O}(\varkappa^2) = S_{\mathrm{HH}} + \mathcal{O}(\varkappa^2). \end{aligned}$$

2.3.3. Vertical polarization. In this case, we take $U = H_y$ in equation (24). The first interface condition for H_y at $z = 0$ is the continuity of H_y itself; see (20). The second interface condition is obtained from the continuity of E_x, using the relation

$$\varepsilon(z)E_x = -\frac{\mathrm{i}}{k}\frac{\mathrm{d}H_y}{\mathrm{d}z} \tag{42}$$

that follows from (18), and taking into account that $\varepsilon = 1$ for $z < 0$; see formula (23). Altogether, this yields the following boundary conditions for H_y at $z = 0$:

$$H_y|_{(F)} = H_y|_{(M)}, \qquad \left.\frac{\mathrm{d}H_y}{\mathrm{d}z}\right|_{(F)} = \left.\left(\varepsilon^{-1}\frac{\mathrm{d}H_y}{\mathrm{d}z}\right)\right|_{(M)}. \tag{43}$$

The key difference between these boundary conditions and boundary conditions (37) that we have obtained for the horizontal polarization is the presence of the factor ε^{-1} in the

condition for the normal derivative (i.e. z-derivative) in (43). Because of this factor, for the vertical polarization, the normal derivative of the total field is no longer continuous, and rather undergoes a jump at $z = 0$, which is due to the jump of ε^{-1}; see (43). As the derivative of the incident field (25*b*) is still continuous, the discontinuity appears in the z-derivative of the scattered field:

$$\varepsilon^{-1} \left.\frac{\mathrm{d}H_y^{(\mathrm{sc})}}{\mathrm{d}z}\right|_{(M)} - \left.\frac{\mathrm{d}H_y^{(\mathrm{sc})}}{\mathrm{d}z}\right|_{(F)} = (1-\varepsilon^{-1}) \left.\frac{\mathrm{d}H_y^{(\mathrm{inc})}}{\mathrm{d}z}\right|_{z=0}.$$

Multiplying both sides of this equality by ε and disregarding the quadratic term $(\varepsilon-1)\frac{\mathrm{d}H_y^{(\mathrm{sc})}}{\mathrm{d}z}\big|_{(F)} = \mathcal{O}(\varkappa^2)$ on the left-hand side, we arrive at the inhomogeneous linearized interface condition for the normal derivative of $H_y^{(\mathrm{sc})}$:

$$\left.\frac{\mathrm{d}H_y^{(\mathrm{sc})}}{\mathrm{d}z}\right|_{(M)} - \left.\frac{\mathrm{d}H_y^{(\mathrm{sc})}}{\mathrm{d}z}\right|_{(F)} = (\varepsilon-1) \left.\frac{\mathrm{d}H_y^{(\mathrm{inc})}}{\mathrm{d}z}\right|_{z=0}. \tag{44}$$

Comparing (44) to (34) while taking into account (25*b*), we obtain $R = \mathrm{i}q(\varepsilon-1)$. Hence, according to (35), we obtain (cf formula (39))

$$S_{\mathrm{VV}} \stackrel{\mathrm{def}}{=} C = B = -\frac{r}{4} + \frac{\varepsilon-1}{2} = S_{\mathrm{HH}} Q, \quad \text{where} \quad Q = \frac{K^2-q^2}{k^2}. \tag{45}$$

The true reflection coefficient for this polarization is given by the Fresnel solution [3, chapter I] (cf formula (40))

$$S_{\mathrm{VV}}^{(\mathrm{exact})} = \frac{\tan(\theta_i-\theta_t)}{\tan(\theta_i+\theta_t)} = \frac{\sin\theta_i\cos\theta_i - \sin\theta_t\cos\theta_t}{\sin\theta_i\cos\theta_i + \sin\theta_t\cos\theta_t}, \tag{46}$$

where θ_i and θ_t are defined in (41). As in the case of the horizontal polarization, see section 2.3.2, reflection coefficient (45) derived with the help of the first Born approximation can also be obtained by linearization of the exact reflection coefficient (46) with respect to $\varkappa$:

$$S_{\mathrm{VV}}^{(\mathrm{exact})} = \frac{\varepsilon - (1+\varkappa k^2/q^2)^{1/2}}{\varepsilon + (1+\varkappa k^2/q^2)^{1/2}} = -\frac{1}{4}\frac{k^2}{q^2}\varkappa + \frac{\varepsilon-1}{2} + \mathcal{O}(\varkappa^2) = S_{\mathrm{VV}} + \mathcal{O}(\varkappa^2),$$

where we have used the same transformations as in section 2.3.2.

The plots in figure 2(a) show the exact and linearized reflection coefficients for both polarizations, as well as the polarization ratio Q, calculated using the first Born approximation and according to the Fresnel formulae. As expected, the accuracy of the first Born approximation decreases as the value of $(\varepsilon-1)$ increases. Note that the typical values of the refractive index $\sqrt{\varepsilon}$ are between 1 and 2 [3, chapters I and II].

Remark. The expression for the polarization ratio Q in formula (45) indicates that the scattered field in the vertical polarization vanishes if $|K| = |q|$, i.e. if the incidence angle is $\pi/4$. In other words, the Brewster angle in the linearized framework is equal to $\pi/4$. This should be expected for a weakly refractive material, in which the direction of the transmitted ray is close to that of the incident one (i.e. $|\theta_i - \theta_t| \sim \varkappa$; see formula (41)), and hence perpendicular to the direction of the reflected ray (see, e.g., [3, chapter I]).

2.3.4. Discussion of the isotropic case. Hereafter, we restrict our analysis to the scattering of plane transverse waves off a plane interface, so that the tangential components of the wave vectors for the incident, transmitted and reflected fields are the same. Under these assumptions, the reflection angle is known, and hence the reflection coefficients computed in sections 2.3.2 and 2.3.3 (and sections 2.4 and 2.5 for other types of scatterers) already take into account the transformation between the coordinate systems used for representing the incident field and the

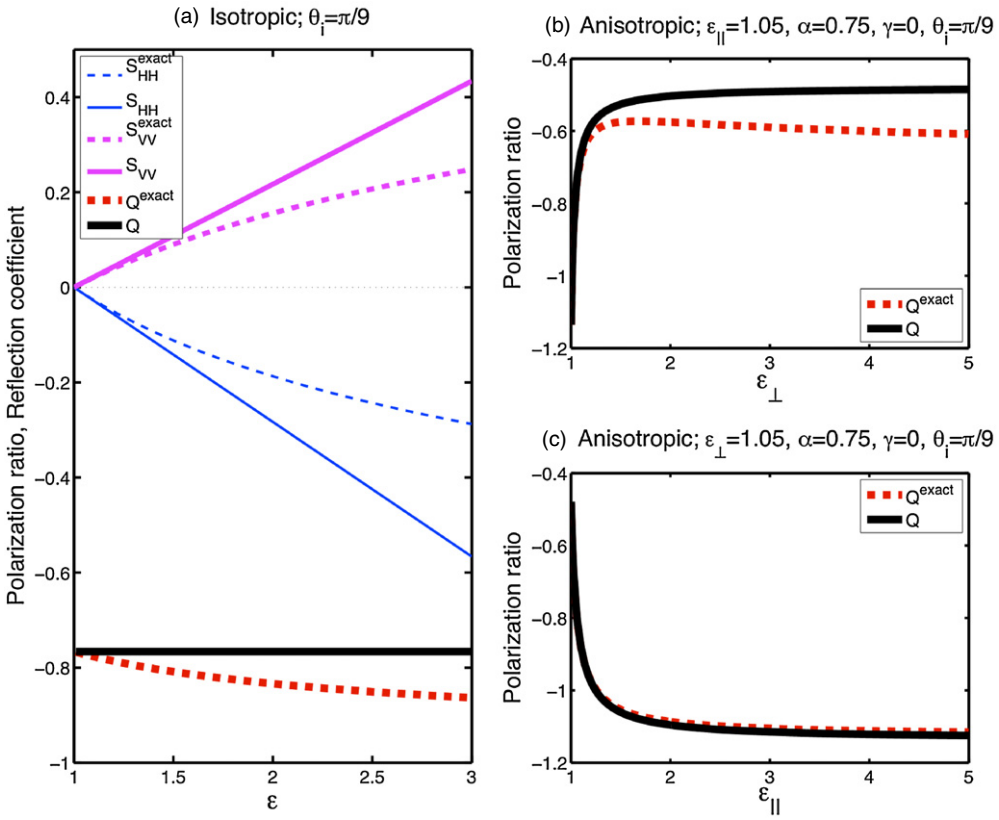

Figure 2. Reflection coefficients and polarization ratios for the linearized and full formulation: (a) lossless isotropic dielectric; (b) and (c): lossless birefringent dielectric with $\varepsilon_\perp$ and $\varepsilon_\parallel$ as independent variables, respectively.

reflected field; see the discussion after equation (13). Moreover, as we are considering only genuine plane waves, we can attribute both $\boldsymbol{E}^{(\mathrm{sc})}$ and $\boldsymbol{E}^{(\mathrm{inc})}$ in formula (13) to the same location right at the interface, rather than to different spatial locations in the far field (that allow one to approximate a more general wave form by a plane wave). Therefore, we may actually leave out the common phase ϕ_0, see (16*a*), that takes into account the propagation distance/time, and directly associate the reflection coefficients we compute with the corresponding entries of the scattering matrix $\mathcal{S}$. This approach will be adopted for the rest of the paper.

The analysis of the reflection coefficients (39) and (45) shows that scattering off a perfect isotropic dielectric yields only one degree of freedom in the scattering matrix $\mathcal{S}$ of (15). At the same time, the reflection coefficients for two polarizations, S_{HH} and S_{VV}, differ by a factor of Q, see formula (45), that does not depend on the material properties at all. Therefore, when this type of scattering material is assumed, the only quantity that can be reconstructed from measurements is $\varepsilon - 1$, which also happens to be the only physical characteristic of the target, regardless of the received polarization(s). If, however, there is a mismatch between the observations and the predictions of the model (e.g., if the ratio of the received co-polarized signals differs substantially from Q, or if significant cross-polarized components are detected), then the use of a more comprehensive model for the scattering material may be justified (see sections 2.4 and 2.5).

2.4. Perfect birefringent dielectric

2.4.1. Governing equations. A perfect (i.e. lossless) anisotropic medium is characterized by the dielectric tensor $\boldsymbol{\varepsilon}$ that relates the components of $\boldsymbol{D}$ and $\boldsymbol{E}$:

$$D_i = \varepsilon_{ij} E_j, \quad i, j = x, y, z, \tag{47}$$

while $\boldsymbol{\sigma}$ is a zero tensor, so that $\tilde{\boldsymbol{D}}$ in (19) is still the same as $\boldsymbol{D}$. For a birefringent material (i.e. a uniaxial crystal), there exists a coordinate system x', y', z', in which the tensor $\boldsymbol{\varepsilon}$ is diagonal and relation (47) simplifies to

$$D_{x'} = \varepsilon_\perp E_{x'}, \quad D_{y'} = \varepsilon_\perp E_{y'}, \quad D_{z'} = \varepsilon_\parallel E_{z'}. \tag{48}$$

Let $\boldsymbol{c}$ be a unit vector along the z' axis, and let α, β and γ be its x, y and z components, respectively (see figure 1). The components of a unit vector are related by

$$\alpha^2 + \beta^2 + \gamma^2 = 1. \tag{49}$$

Then, the entries of the tensor $\boldsymbol{\varepsilon}$ become (see [22, 23])

$$\begin{aligned} &\varepsilon_{xx} = \varepsilon_\perp + \alpha^2 \Delta\varepsilon, \quad \varepsilon_{yy} = \varepsilon_\perp + \beta^2 \Delta\varepsilon, \quad \varepsilon_{zz} = \varepsilon_\perp + \gamma^2 \Delta\varepsilon, \\ &\varepsilon_{xy} = \varepsilon_{yx} = \alpha\beta\Delta\varepsilon, \quad \varepsilon_{xz} = \varepsilon_{zx} = \alpha\gamma\Delta\varepsilon, \quad \varepsilon_{yz} = \varepsilon_{zy} = \beta\gamma\Delta\varepsilon, \end{aligned} \tag{50}$$

where $\Delta\varepsilon = \varepsilon_\parallel - \varepsilon_\perp$. The diagonal terms in (50) are $\mathcal{O}(1)$, while the off-diagonal terms are $\mathcal{O}(\varkappa)$ (cf the first relation in formula (22)).

The isotropic case considered in section 2.3 is characterized by $\Delta\varepsilon = 0$. There, the off-diagonal terms in (50) vanish and the two basic polarizations (horizontal and vertical) in the system (19) separate. They are described individually by equation (24) for E_y and H_y, respectively. If $\Delta\varepsilon \neq 0$ though, then the two polarizations remain coupled. However, the treatment of this case is greatly simplified in the presence of a small parameter $\varkappa$. Namely, our assumption that the dielectric is weak implies that the coupling terms are small. For the case of weak coupling, it still makes sense to use E_y and H_y as the unknowns in the problem, because it simplifies the analysis of the Born approximation and makes the comparison to the isotropic case (equation (24)) easier.

To reduce the system (19) to two equations for E_y and H_y, we will use the inverse dielectric tensor $\boldsymbol{\eta}$ defined as

$$E_i = \eta_{ij} D_j, \quad i, j = x, y, z. \tag{51}$$

The entries of this tensor, *accurate to* $\mathcal{O}(\varkappa)$, are

$$\begin{aligned} &\eta_{xx} = 1/\varepsilon_{xx}, \quad \eta_{yy} = 1/\varepsilon_{yy}, \quad \eta_{zz} = 1/\varepsilon_{zz}, \\ &\eta_{xy} = \eta_{yx} = -\varepsilon_{xy}, \quad \eta_{xz} = \eta_{zx} = -\varepsilon_{xz}, \quad \eta_{yz} = \eta_{zy} = -\varepsilon_{yz}, \end{aligned} \tag{52}$$

which can be proven by observing that all entries of the tensor $\boldsymbol{\varepsilon} \cdot \boldsymbol{\eta} - \mathcal{I}$ are $o(\varkappa)$. Then, we eliminate all field components except E_y and H_y from the system (19) as follows.

(i) Dependence (27) on the x coordinate is assumed for all field components, so in the system (19), we replace $\partial/\partial x$ by $\mathrm{i}K$ and $\partial/\partial z$ by $\mathrm{d}/\mathrm{d}z$, respectively. This allows us to explicitly express the components D_x, D_z, H_x and H_z via E_y, H_y and their derivatives with respect to z:

$$D_x = -\frac{\mathrm{i}}{k}\frac{\mathrm{d}H_y}{\mathrm{d}z}, \qquad D_z = -\frac{K}{k} H_y, \tag{53a}$$

$$H_x = \frac{\mathrm{i}}{k}\frac{\mathrm{d}E_y}{\mathrm{d}z}, \qquad H_z = \frac{K}{k} E_y. \tag{53b}$$

(ii) Formulae (53*b*) are substituted into the expression for D_y in (19), which yields

$$D_y = -\frac{1}{k^2}\left(\frac{\mathrm{d}^2 E_y}{\mathrm{d}z^2} - K^2 E_y\right). \tag{54}$$

(iii) Equations (53*a*) and (54) are substituted into formula (51), which leads to the following expressions for E_x and E_z:

$$E_x = -\eta_{xx}\frac{\mathrm{i}}{k}\frac{\mathrm{d}H_y}{\mathrm{d}z} - \eta_{xy}\frac{1}{k^2}\left(\frac{\mathrm{d}^2 E_y}{\mathrm{d}z^2} - K^2 E_y\right) - \eta_{xz}\frac{K}{k}H_y, \tag{55a}$$

$$E_z = -\eta_{zz}\frac{K}{k}H_y - \eta_{xz}\frac{\mathrm{i}}{k}\frac{\mathrm{d}H_y}{\mathrm{d}z} - \eta_{yz}\frac{1}{k^2}\left(\frac{\mathrm{d}^2 E_y}{\mathrm{d}z^2} - K^2 E_y\right), \tag{55b}$$

whereas for E_y, we obtain

$$\left(\eta_{yy}\frac{\mathrm{d}^2}{\mathrm{d}z^2} + k^2 - K^2\eta_{yy}\right)E_y = -k\left(\mathrm{i}\eta_{xy}\frac{\mathrm{d}}{\mathrm{d}z} + K\eta_{yz}\right)H_y. \tag{56}$$

(iv) Expressions (55) are substituted into the y component of the Faraday law in (19) (the equation that relates E_x, E_z and H_y). After simplifications, we arrive at

$$\left(\eta_{xx}\frac{\mathrm{d}^2}{\mathrm{d}z^2} + k^2 - K^2\eta_{zz}\right)H_y - 2\mathrm{i}\eta_{xz}K\frac{\mathrm{d}H_y}{\mathrm{d}z} = -\frac{\mathrm{i}}{k}\left(i\eta_{yz}K - \eta_{xy}\frac{\mathrm{d}}{\mathrm{d}z}\right)\left(\frac{\mathrm{d}^2 E_y}{\mathrm{d}z^2} - K^2 E_y\right). \tag{57}$$

Note that the isotropic equation (24) can be derived from equation (56), or from equation (57), by setting $\Delta\varepsilon = 0$ in formulae (50) and (52). As will be seen in sections 2.4.2 and 2.4.3, equations (56) and (57) are particularly well suited for computing the scattered field because of the way they couple the components E_y and H_y. Specifically, for electromagnetic fields represented in the form (25*a*), it appears very convenient to carry out the Born approximation in two stages: first decouple equations (56) and (57) from one another, and then linearize the resulting individual equations.

The system (56), (57) will also require boundary conditions at $z = 0$; see (20). The boundary conditions will be obtained with the help of relations for H_x and E_x in formulae (53*b*) and (55*a*). In the isotropic case, expression (55*a*) with (52) taken into account reduces to (42), as expected. In the anisotropic case, the right-hand side of expression (55*a*) will be responsible for the inhomogeneous boundary conditions (similar to (42) and (44) in the isotropic case) for the vertical polarization of the scattered field[8].

Let us now consider the two basic polarizations of the incident wave separately. For each one, the scattered field can also be polarized either vertically or horizontally.

2.4.2. Horizontal polarization of the incident wave. In this case, the component H_y is present only in the scattered field; hence, $H_y = \mathcal{O}(\varkappa)$ (see (25*c*)). Therefore, the right-hand side of equation (56) appears $\mathcal{O}(\varkappa^2)$ because according to (50) and (52), $\eta_{xy} \sim \Delta\varepsilon = \mathcal{O}(\varkappa)$ and $\eta_{yz} \sim \Delta\varepsilon = \mathcal{O}(\varkappa)$. As such, this right-hand side can be neglected, and the co-polarized scattering for the horizontal incident polarization is described by

$$\left(\eta_{yy}\frac{\mathrm{d}^2}{\mathrm{d}z^2} + k^2 - K\eta_{yy}\right)E_y = 0.$$

[8] The inhomogeneous boundary condition will apply to the co-polarized component of the scattered field when the incident field is polarized vertically, and to the cross-polarized component of the scattered field when the incident field is polarized horizontally.

This equation can be transformed into

$$\hat{L}E_y = \frac{\eta_{yy}-1}{q^2}\left(K^2 - \frac{\mathrm{d}^2}{\mathrm{d}z^2}\right)E_y, \tag{58}$$

where the operator $\hat{L}$ is defined in (28). Linearization of (58) according to (25) yields

$$\frac{1}{E_{0y}^{(\mathrm{inc})}}\hat{L}E_y^{(\mathrm{sc})} = \frac{(\eta_{yy}-1)k^2}{q^2}\theta(z)\,\mathrm{e}^{\mathrm{i}qz}, \tag{59}$$

which coincides with equation (28) for $r = -(\eta_{yy}-1)k^2/q^2$ and $u_0 = E_{0y}^{(\mathrm{inc})}$.

Since in the co-polarized case the scattered wave is also polarized horizontally, E_y and H_x must be continuous at $z = 0$; see (20), where the expression for H_x is given by the first equality of (53*b*). Recalling that the incident field is continuous at the interface along with its normal derivative, we obtain the continuity of $E_y^{(\mathrm{sc})}$ and $\frac{\mathrm{d}E_y^{(\mathrm{sc})}}{\mathrm{d}z}$:

$$E_y^{(\mathrm{sc})}\big|_{(F)} = E_y^{(\mathrm{sc})}\big|_{(M)}, \quad \left.\frac{\mathrm{d}E_y^{(\mathrm{sc})}}{\mathrm{d}z}\right|_{(F)} = \left.\frac{\mathrm{d}E_y^{(\mathrm{sc})}}{\mathrm{d}z}\right|_{(M)}, \tag{60}$$

so that in formula (34) we have $R = 0$. Interface conditions (60) are the same as (38) in the isotropic case. Using (35) for $E_y^{(\mathrm{sc})}$, we obtain the following reflection coefficient:

$$S_{\mathrm{HH}} = \frac{1}{4}\frac{k^2}{q^2}(\eta_{yy}-1). \tag{61}$$

For $\Delta\varepsilon = 0$, formula (61), with the help of (52), reduces to the isotropic expression in (39), as expected.

For the cross-polarized scattering, i.e. the vertical polarization of the scattered wave, we linearize equation (57) taking into account that $H_y^{(\mathrm{inc})} = 0$ and hence $H_y = H_y^{(\mathrm{sc})} = \mathcal{O}(\varkappa)$ according to (25*c*). Thus, on the left-hand side we may replace η_{xx} and η_{zz} by 1. The remaining off-diagonal terms of $\boldsymbol{\eta}$ are $\mathcal{O}(\varkappa)$; hence, we drop the η_{xz} term on the left-hand side and replace E_y by $E_y^{(\mathrm{inc})}$ on the right-hand side. This yields

$$\left(\frac{\mathrm{d}^2}{\mathrm{d}z^2} + q^2\right)H_y^{(\mathrm{sc})} = -\frac{\mathrm{i}}{k}\left(\mathrm{i}\eta_{yz}K - \eta_{xy}\frac{\mathrm{d}}{\mathrm{d}z}\right)\left(\frac{\mathrm{d}^2E_y^{(\mathrm{inc})}}{\mathrm{d}z^2} - K^2E_y^{(\mathrm{inc})}\right). \tag{62}$$

Equation (62) can be transformed into

$$\frac{1}{E_{0y}^{(\mathrm{inc})}}\hat{L}H_y^{(\mathrm{sc})} = \frac{k}{q}\left(\eta_{xy} - \frac{K}{q}\eta_{yz}\right)\theta(z)\,\mathrm{e}^{\mathrm{i}qz}. \tag{63}$$

As the polarization of the scattered field is vertical, $H_y = H_y^{(\mathrm{sc})}$ and E_x must be continuous at $z = 0$; see (20). We use formula (55*a*) for E_x to express the interface conditions via the y-components of the fields. Using $H_y^{(\mathrm{sc})} = \mathcal{O}(\varkappa)$ and recalling that the off-diagonal terms of $\boldsymbol{\eta}$ are also $\mathcal{O}(\varkappa)$, we can set $\eta_{xx} = 1$ in the first term and drop the third term on the right-hand side of that relation. Thus, we arrive at the following interface condition for the normal derivative of $H_y^{(\mathrm{sc})}$:

$$-\frac{\mathrm{i}}{k}\left.\frac{\mathrm{d}H_y^{(\mathrm{sc})}}{\mathrm{d}z}\right|_{(F)} = -\frac{\mathrm{i}}{k}\left.\frac{\mathrm{d}H_y^{(\mathrm{sc})}}{\mathrm{d}z}\right|_{(M)} + \eta_{xy}E_{0y}^{(\mathrm{inc})}. \tag{64}$$

It is inhomogeneous due to the second term on the right-hand side of (55*a*) (cf (44)).

To define the cross-polarized reflection coefficient for this case, we use the following convention: if the scattered field in vacuum is given by $H_y^{(\mathrm{sc})} = H_{0y}^{(\mathrm{sc})}\,\mathrm{e}^{\mathrm{i}Kx-\mathrm{i}qz}$ (see equations (27) and (33)), then the reflection coefficient will be

$$S_{\mathrm{VH}} \stackrel{\mathrm{def}}{=} H_{0y}^{(\mathrm{sc})}\big/E_{0y}^{(\mathrm{inc})}. \tag{65}$$

Next, we introduce the notation

$$G^{\pm} \stackrel{\text{def}}{=} -\left(\eta_{xy} \pm \frac{K}{q}\eta_{yz}\right) = \Delta\varepsilon\left(\alpha\beta \pm \frac{K}{q}\beta\gamma\right) \tag{66}$$

(see (52) for the components of $\boldsymbol{\eta}$) and match equation (63) to (28), which yields $u_0 \equiv E_{0y}^{(\text{inc})}$ and $r = kG^{-}/q$ (note the minus sign in (66)). We also match the interface condition (64) to the second condition (34), which yields $R = -\mathrm{i}k\eta_{xy}$. Substituting these values of r and R into (35), we express the cross-polarized reflection coefficient defined by (65) as

$$S_{\text{VH}} = \frac{1}{4}\frac{k}{q}G^{+}. \tag{67}$$

2.4.3. Vertical polarization of the incident wave. We start with the co-polarized scattering again. For this case, we have $E_y^{(\text{inc})} = 0$ and, consequently, $E_y = E_y^{(\text{sc})} = \mathcal{O}(\varkappa)$. As $\eta_{yz} \sim \eta_{xy} = \mathcal{O}(\varkappa)$, the right-hand side of equation (57) can be dropped, making this equation homogeneous:

$$\left(\eta_{xx}\frac{\mathrm{d}^2}{\mathrm{d}z^2} + k^2 - K^2\eta_{zz}\right)H_y - 2\mathrm{i}\eta_{xz}K\frac{\mathrm{d}H_y}{\mathrm{d}z} = 0.$$

Linearization of this equation gives

$$\frac{1}{H_{0y}^{(\text{inc})}}\hat{L}H_y^{(\text{sc})} = \left((\eta_{xx}-1) + \frac{K^2}{q^2}(\eta_{zz}-1) - 2\eta_{xz}\frac{K}{q}\right)\theta(z)\,\mathrm{e}^{\mathrm{i}qz}, \tag{68}$$

where $H_{0y}^{(\text{inc})}$ is the amplitude of the incident wave. The interface conditions for this co-polarized case require the continuity of H_y and E_x at $z = 0$. Given the continuity of the incident field along with its normal derivative, the second equation of (20*b*) yields the continuity of $H_y^{(\text{sc})}$, while for E_x we employ formula (55*a*) and after the linearization obtain

$$-\frac{\mathrm{i}}{k}\frac{\mathrm{d}H_y^{(\text{sc})}}{\mathrm{d}z}\bigg|_{(F)} = -\frac{\mathrm{i}}{k}\frac{\mathrm{d}H_y^{(\text{sc})}}{\mathrm{d}z}\bigg|_{(M)} + \frac{q}{k}(\eta_{xx}-1)H_{0y}^{(\text{inc})} - \frac{K}{k}\eta_{xz}H_{0y}^{(\text{inc})}. \tag{69}$$

Similarly to the isotropic case, see formula (44), the normal derivative of $H_y^{(\text{sc})}$ is discontinuous at the interface. Comparing (68) and (69) to (28) and (34), we obtain

$$r = -\left((\eta_{xx}-1) + \frac{K^2}{q^2}(\eta_{zz}-1) - 2\eta_{xz}\frac{K}{q}\right) \text{ and } R = \mathrm{i}K\eta_{xz} - \mathrm{i}q(\eta_{xx}-1).$$

Then, using formula (35), we obtain

$$S_{\text{VV}} = -\frac{1}{4}\left((\eta_{xx}-1) - \frac{K^2}{q^2}(\eta_{zz}-1)\right). \tag{70}$$

For $\Delta\varepsilon = 0$, formula (70), with the help of (52), reduces to the isotropic expression in (45), as expected.

The cross-polarized field in this case is governed by the linearized equation (56):

$$\left(\frac{\mathrm{d}^2}{\mathrm{d}z^2} + q^2\right)E_y^{(\text{sc})} = -k\left(\mathrm{i}\eta_{xy}\frac{\mathrm{d}}{\mathrm{d}z} + K\eta_{yz}\right)H_y^{(\text{inc})},$$

which can be transformed into

$$\frac{1}{H_{0y}^{(\text{inc})}}\hat{L}E_y^{(\text{sc})} = \frac{k}{q^2}\left(q\eta_{xy} - K\eta_{yz}\right)\theta(z)\,\mathrm{e}^{\mathrm{i}qz}. \tag{71}$$

Remarkably, the value of r in (71) and (63) is the same, $r = kG^{-}/q$, where G^{-} is defined by (66). The difference between the cross-polarized case of section 2.4.2 and the cross-polarized

case considered here is in the boundary conditions. Indeed, for the current cross-polarized case, we require the continuity of E_y and H_x at $z = 0$, which translates into the homogeneous boundary conditions (60) by taking into account that $E_y = E_y^{(\mathrm{sc})}$ and using the first equation of (53*b*) for H_x. Hence, $R = 0$, and using formula (35) for $E_y^{(\mathrm{sc})}$ with $u_0 \equiv H_{0y}^{(\mathrm{inc})}$, we arrive at the reflection coefficient

$$S_{\mathrm{HV}} = -\frac{1}{4}\frac{k}{q}G^-, \tag{72}$$

which is different from (67). In formula (72), S_{HV} is defined similarly to (65),

$$S_{\mathrm{HV}} \stackrel{\mathrm{def}}{=} E_{0y}^{(\mathrm{sc})}/H_{0y}^{(\mathrm{inc})} \quad \text{provided that} \quad E_y^{(\mathrm{sc})} = E_{0y}^{(\mathrm{sc})}\,\mathrm{e}^{\mathrm{i}Kx-\mathrm{i}qz} \quad \text{for} \quad z < 0.$$

2.4.4. Scattering coefficients for a perfect birefringent dielectric. For future reference, we present here the expressions for the reflection coefficients given by (61), (70), (67) and (72) in the following form (expressions (50), (52) and (66) have also been used):

$$\begin{aligned}
S_{\mathrm{HH}} &= -\frac{1}{4}\frac{k^2}{q^2}(\varepsilon_\perp - 1 + \beta^2\Delta\varepsilon),\\
S_{\mathrm{VV}} &= \frac{1}{4}\left((\varepsilon_\perp - 1 + \alpha^2\Delta\varepsilon) - \frac{K^2}{q^2}(\varepsilon_\perp - 1 + \gamma^2\Delta\varepsilon)\right),\\
S_{\mathrm{HV}} &= -\frac{1}{4}\frac{k}{q}\left(\alpha - \frac{K}{q}\gamma\right)\beta\Delta\varepsilon,\\
S_{\mathrm{VH}} &= \frac{1}{4}\frac{k}{q}\left(\alpha + \frac{K}{q}\gamma\right)\beta\Delta\varepsilon.
\end{aligned} \tag{73}$$

2.4.5. Scattering off the basal plane. We start analyzing particular geometries by assuming that the interface between the vacuum and material is normal to the optical axis, in which case we say that it coincides with the so-called basal plane. Substituting $\alpha = 0$, $\beta = 0$ and $\gamma = 1$ (see figure 1) into equations (73), we obtain the following expressions for the reflection coefficients:

$$\begin{aligned}
&S_{\mathrm{HH}} = -\frac{1}{4}\frac{k^2}{q^2}(\varepsilon_\perp - 1),\\
&S_{\mathrm{VV}} = S_{\mathrm{HH}}Q, \quad \text{where} \quad Q = \frac{1}{k^2}\left(K^2\frac{\varepsilon_\parallel - 1}{\varepsilon_\perp - 1} - q^2\right),\\
&S_{\mathrm{VH}} = 0, \quad S_{\mathrm{HV}} = 0.
\end{aligned} \tag{74}$$

Comparing the values of Q in formulae (74) and (45), we see that unlike in the isotropic case (see figure 2(a)), the ratio of the co-polarized reflection coefficients now depends on the material properties. Indeed, while the quantity Q in (45) depends only on the incident angle, in (74) it may assume any real value, depending on $(\varepsilon_\perp - 1)$ and $(\varepsilon_\parallel - 1)$. Therefore, this scattering configuration has two degrees of freedom rendered by the real-valued reflection coefficients S_{HH} and S_{VV}.

Once the co-polarized channels S_{HH} and S_{VV} have been defined according to (74), one can look into the possibility of reconstructing the material parameters $\varepsilon_\perp$ and $\varepsilon_\parallel$ while interpreting S_{HH} and S_{VV} as the given data. It turns out that the system (74) can be solved with respect to $\varepsilon_\perp$ and $\varepsilon_\parallel$ for any values of the observables S_{HH} and S_{VV}. However, not every choice of the

input data results in a physically feasible solution. In particular, the value of $Q = S_{VV}/S_{HH}$ should satisfy the condition

$$Q + \frac{q^2}{k^2} > 0 \tag{75}$$

in order for the susceptibilities to be positive:

$$\varepsilon_\perp - 1 > 0 \quad \text{and} \quad \varepsilon_\parallel - 1 > 0. \tag{76}$$

If condition (75) is not satisfied, then at least one of the requirements on the material parameters in (76) will not be met.

2.4.6. Arbitrary direction of the optical axis. The analysis of the last two equations in (73) shows that the cross-polarized channels are nonzero if $\beta \neq 0$ and $\beta \neq 1$, i.e. when the optical axis is neither parallel nor perpendicular to the plane of incidence (note that the basal plane case considered in section 2.4.5 corresponds to $\beta = 0$, i.e. the optical axis is parallel to the incidence plane, and thus provides only co-polarized scattering channels; see (74)). The cross-polarized channels are also proportional to $\Delta\varepsilon$, which once again shows that they vanish in the isotropic case. The ratio of the two off-diagonal entries of the scattering matrix is given by

$$\frac{S_{HV}}{S_{VH}} = -\frac{q\alpha - K\gamma}{q\alpha + K\gamma}.$$

This expression can help identify the individual effects of α and γ. If $\alpha = 0$, then the off-diagonal entries are equal. If $\gamma = 0$, i.e. the optical axis is parallel to the interface, then the sum of the off-diagonal entries is zero. In either of these two cases, the overall number of degrees of freedom is 3, otherwise, i.e. when $\alpha\beta\gamma \neq 0$, it is 4.

The ratio Q of two co-polarized reflection coefficients for the arbitrary direction of the optical axis differs from that given in formula (74), but still depends on $\Delta\varepsilon$:

$$\begin{aligned} Q = \frac{S_{VV}}{S_{HH}} &= \frac{1}{k^2(\eta_{yy} - 1)}(K^2(\eta_{zz} - 1) - q^2(\eta_{xx} - 1)) \\ &= \frac{1}{k^2}\left(K^2\frac{\varepsilon_\perp - 1 + \gamma^2\Delta\varepsilon}{\varepsilon_\perp - 1 + \beta^2\Delta\varepsilon} - q^2\frac{\varepsilon_\perp - 1 + \alpha^2\Delta\varepsilon}{\varepsilon_\perp - 1 + \beta^2\Delta\varepsilon}\right). \end{aligned} \tag{77}$$

The plots in figures 2(b) and (c) illustrate how Q depends on $\varepsilon_\perp$ and $\varepsilon_\parallel$ for $\theta_i = \pi/9$. The exact formulation is made according to [22]. Similarly to the reflection coefficients in figure 2(a), the linearized and exact values are close if $|\varepsilon_\perp - 1| \ll 1$ and $|\varepsilon_\parallel - 1| \ll 1$.

2.4.7. Discussion of the lossless birefringent medium. Compared to the isotropic case characterized by the scalar dielectric coefficient ε (section 2.3), the case of a perfect uniaxial dielectric is controlled by four parameters: $\varepsilon_\perp$, $\varepsilon_\parallel$, α and γ (note that β is not an independent quantity due to relation (49)). Depending on the particular geometry, this case may provide two ($\gamma = 1$, section 2.4.5), three ($\alpha = 0$, $\beta\gamma \neq 0$ or $\gamma = 0$, $\alpha\beta \neq 0$) or four ($\alpha\beta\gamma \neq 0$) degrees of freedom (section 2.4.6). However, the mere availability of the correct number of degrees of freedom does not, generally speaking, guarantee that the problem of reconstructing the material properties from reflection coefficients has a solution for any angle of incidence and any input data (i.e. any arbitrary values of the observable quantities S_{HH}, S_{VV}, S_{HV} and S_{VH}).

The issue of solvability of the aforementioned problem is addressed by the following.

Theorem 1. *Equations (73) can be solved with respect to* $\varepsilon_\perp$, $\varepsilon_\parallel$, α *and* γ *for the given* S_{HH}, S_{VV}, S_{HV}, S_{VH} *and* θ_i *if and only if*

$$(S_{\mathrm{VV}} + VS_{\mathrm{HH}})^2 \geqslant 4VS_{\mathrm{HV}}S_{\mathrm{VH}}, \tag{78}$$

where

$$V = \frac{q^2 - K^2}{k^2} = \cos^2\theta_i - \sin^2\theta_i = \cos 2\theta_i,$$

and θ_i *is the angle of incidence defined in (41).*

Theorem 1 is proved in Appendix B. Theorem 1 shows, in particular, that for the linearized scattering off a plane interface between the vacuum and a lossless birefringent dielectric, the inverse problem does not have a solution for all possible combinations of reflection coefficients; see (78). It is not clear ahead of time what may be causing this limitation of solvability: whether it is the type of the material that we have chosen or the linearization itself. We address this question in Appendix C by conducting numerical simulations for the exact formulation of the direct scattering problem. It turns out that even with no linearization, there are still regions in the space of reflection coefficients for which there is no solution. Moreover, if in the case of weak scattering (when the linearization applies) neither the linearized nor the original problem happens to have a solution, then the regions of no solution for both problems seem to coincide. Hence, the limitation of solvability of the linearized inverse problem shall be attributed to the type of the target material rather than to the first Born approximation.

2.5. Isotropic and anisotropic lossy dielectric

2.5.1. Modified permittivity tensor in the presence of a finite conductivity. First, we consider the case of an isotropic lossy dielectric, i.e. $\boldsymbol{\varepsilon} = \varepsilon\mathcal{I}$, $\boldsymbol{\sigma} = \sigma\mathcal{I}$, where $\varepsilon > 0$ and $\sigma > 0$ are scalars. Then, the propagation is governed by equations (18) supplemented by the material relations

$$\boldsymbol{D} = \varepsilon\boldsymbol{E} \quad \text{and} \quad \boldsymbol{j} = \sigma\boldsymbol{E}. \tag{79}$$

Given (79), the second equation of (18) transforms into

$$\nabla \times \boldsymbol{H} = -\mathrm{i}k\tilde{\varepsilon}\boldsymbol{E},$$

where (cf formula (11))

$$\tilde{\varepsilon} = \varepsilon + \mathrm{i}\frac{4\pi\sigma}{\omega} = 1 + (\varepsilon - 1) + \mathrm{i}\frac{4\pi\sigma}{\omega}. \tag{80}$$

This is equivalent to the previously considered case of a perfect isotropic dielectric (section 2.3) with a redefined dielectric constant. The applicability of the first Born approximation (see section 2.3.1) requires that the conductivity term in expression (80) be small, or $4\pi\sigma/\omega \sim \varkappa \ll 1$; see (22). If this condition is satisfied, then all the formulae in section 2.3 remain valid, with ε replaced by $\tilde{\varepsilon}$.

We will now extend this consideration to anisotropic permittivity and conductivity. For the latter, we assume a uniaxial model described by the parameters $\sigma_\perp, \sigma_\parallel, \alpha_\sigma, \beta_\sigma$ and γ_σ, similarly to the model of the dielectric tensor described in section 2.4.1. Hence, the representation of the conductivity tensor in the coordinates of figure 1 will be given by formula (50) with $(\sigma_\perp, \sigma_\parallel)$ substituted for $(\varepsilon_\perp, \varepsilon_\parallel)$ and $(\alpha_\sigma, \beta_\sigma, \gamma_\sigma)$ substituted for (α, β, γ). Given this representation and the linearity of relations (79), we can derive the following tensor counterpart of the scalar formula (80):

$$\tilde{\boldsymbol{\varepsilon}} = \boldsymbol{\varepsilon} + \mathrm{i}\frac{4\pi}{\omega}\boldsymbol{\sigma}. \tag{81}$$

Next, note that the reflection coefficients in (73) are linear functions of susceptibilities $(\varepsilon_\parallel - 1)$ and $(\varepsilon_\perp - 1)$ (note that $\Delta\varepsilon \equiv (\varepsilon_\parallel - 1) - (\varepsilon_\perp - 1)$), which is in agreement with the first Born approximation being a linear perturbation method with the susceptibilities playing the role of small parameters. Therefore, with the conductivities taken into account, the new scattering amplitudes can be calculated by simple substitution rules, e.g., for S_{HH}, we have

$$\begin{gathered} S_{\mathrm{HH}} = -\frac{1}{4}\frac{k^2}{q^2}((\varepsilon_\perp - 1) + \beta^2\Delta\varepsilon) \\ \Downarrow \\ \tilde{S}_{\mathrm{HH}} = -\frac{1}{4}\frac{k^2}{q^2}\left((\varepsilon_\perp - 1) + \beta^2\Delta\varepsilon + \mathrm{i}\frac{4\pi}{\omega}\left(\sigma_\perp + \beta_\sigma^2\Delta\sigma\right)\right), \end{gathered} \tag{82}$$

where $\Delta\sigma = \sigma_\parallel - \sigma_\perp$.

2.5.2. Isotropic permittivity and isotropic conductivity. The reflection coefficients (39) and (45), modified by the foregoing procedure, contain the factor of $(\tilde{\varepsilon} - 1)$, see (80), and thus become complex. Their complexity affects the phase of the reflected wave. However, the *ratio* of the reflection coefficients for the vertical and horizontal polarizations is still equal to the same quantity Q defined in (45). Moreover, the phase difference between the two reflection coefficients, or CPD, remains unchanged, i.e. equal to zero. As such, despite the changes in the values of the reflection coefficients due to a finite conductivity, this case still has only one degree of freedom, the same as the case of a perfect isotropic dielectric (see section 2.3.4).

2.5.3. Anisotropic permittivity and isotropic conductivity: reflection from basal plane. We analyze the effect of conductivity on the scattering amplitudes obtained in section 2.4.5 assuming that the conductivity is isotropic, i.e. $\sigma_\perp = \sigma_\parallel = \sigma$. In this case, the value of Q in (74) should be replaced by

$$Q = \frac{1}{k^2}\left(K^2\frac{\varepsilon_\parallel - 1 + (\mathrm{i}4\pi\sigma)/\omega}{\varepsilon_\perp - 1 + (\mathrm{i}4\pi\sigma)/\omega} - q^2\right). \tag{83}$$

The new quantity Q defined by (83) depends on σ provided that $\varepsilon_\perp \neq \varepsilon_\parallel$. This means that the conductivity σ brings along a new degree of freedom to the scattering matrix. Qualitatively, the difference compared to the lossless case (74) is that the ratio of the co-polarized scattering amplitudes becomes complex, which introduces a phase shift between the corresponding scattered waves (i.e. a nonzero CPD). In particular, if the incident wave is polarized linearly, then the scattered field will be polarized elliptically.

Similarly to the case of zero conductivity (section 2.4.5), finite conductivity may also result in solutions that are not feasible from the standpoint of physics. For example, expression (83) can be rewritten as

$$Q_1 \stackrel{\mathrm{def}}{=} \frac{k^2}{K^2}\left(Q + \frac{q^2}{k^2}\right) = \frac{\varepsilon_\parallel - 1 + (\mathrm{i}4\pi\sigma)/\omega}{\varepsilon_\perp - 1 + (\mathrm{i}4\pi\sigma)/\omega}. \tag{84}$$

If we assume that the conductivity and susceptibilities are positive, i.e. $\sigma > 0$, $\varepsilon_\perp - 1 > 0$ and $\varepsilon_\parallel - 1 > 0$, then both the real and imaginary parts of the numerator and denominator in the last expression of (84) are positive. It means, in particular, that

$$\mathrm{Re}(Q_1) > 0. \tag{85a}$$

As the imaginary parts of the numerator and denominator are equal, by comparing the absolute values, we obtain

$$\begin{cases} \mathrm{Im}(Q_1) < 0 & \text{if} \quad |Q_1| > 1, \\ \mathrm{Im}(Q_1) > 0 & \text{if} \quad |Q_1| < 1. \end{cases} \tag{85b}$$

Recall that Q (and, consequently, Q_1) is an observable: $Q = S_{VV}/S_{HH}$. If, however, the observed value of Q_1 does not satisfy (85), then the assumption that the conductivity and the two susceptibilities are positive is violated.

2.5.4. Anisotropic permittivity and conductivity. Let $\boldsymbol{P} = ((\varepsilon_\perp - 1), (\varepsilon_\parallel - 1), \alpha, \beta, \gamma)$ be a set of parameters defining the permittivity of the material (section 2.4.1), and $\boldsymbol{C} = (\sigma_\perp, \sigma_\parallel, \alpha_\sigma, \beta_\sigma, \gamma_\sigma)$ be a set of parameters of the material conductivity (section 2.5.1). As shown in section 2.5.1, the effect of a finite 'uniaxial' conductivity can be described by adding imaginary components to the reflection coefficients. For each coefficient, the functional dependence of the imaginary part on the parameters $\boldsymbol{C}$ is similar to that of the real part on $\boldsymbol{P}$ (as illustrated by formula (82)). For the entire matrix of reflection coefficients $\mathcal{S}$ (essentially equivalent to the scattering matrix $\mathcal{S}$ of (15); see section 2.3.4), this functional dependence may be expressed as

$$\mathcal{S} = \mathcal{S}(\boldsymbol{P}, \boldsymbol{C}) = \begin{bmatrix} S_{HH}(\boldsymbol{P}) & S_{HV}(\boldsymbol{P}) \\ S_{VH}(\boldsymbol{P}) & S_{VV}(\boldsymbol{P}) \end{bmatrix} + \mathrm{i}\frac{4\pi}{\omega} \begin{bmatrix} S_{HH}(\boldsymbol{C}) & S_{HV}(\boldsymbol{C}) \\ S_{VH}(\boldsymbol{C}) & S_{VV}(\boldsymbol{C}) \end{bmatrix}. \tag{86}$$

In the first term on the right-hand side of (86), the entries S_{HH}, S_{VH}, S_{HV} and S_{VV} of the matrix are real-valued functions of $\boldsymbol{P}$ defined by (73). In the second term, the same functions are applied to $\boldsymbol{C}$.

It has been shown in section 2.4.6 and Appendix B that for the lossless material, the set of permittivity parameters $\boldsymbol{P}$ provides up to four degrees of freedom to the scattering matrix $\mathcal{S}$ of (86). Further, we note that the real and imaginary parts of $\mathcal{S}$ depend on $\boldsymbol{P}$ and $\boldsymbol{C}$ the same way up to a multiplicative constant $4\pi/\omega$ in front of the imaginary part. Hence, the set of conductivity parameters $\boldsymbol{C}$ provides up to four additional degrees of freedom to the matrix $\mathcal{S}$. Altogether, the combination of $\boldsymbol{P}$ and $\boldsymbol{C}$ provides up to eight degrees of freedom to the complex-valued matrix $\mathcal{S}$.

The result of theorem 1 naturally extends from the lossless material to the lossy material via the following.

Corollary 1. *The permittivity parameters $\boldsymbol{P}$ and the conductivity parameters $\boldsymbol{C}$ can be reconstructed from the given complex-valued entries of the scattering matrix $\mathcal{S}$ of (86) if and only if the inequalities*

$$(\mathrm{Re}(S_{VV}) + V\,\mathrm{Re}(S_{HH}))^2 \geqslant 4V\,\mathrm{Re}(S_{HV})\,\mathrm{Re}(S_{VH}), \tag{87a}$$

$$(\mathrm{Im}(S_{VV}) + V\,\mathrm{Im}(S_{HH}))^2 \geqslant 4V\,\mathrm{Im}(S_{HV})\,\mathrm{Im}(S_{VH}) \tag{87b}$$

hold simultaneously.

Each of inequalities (87*a*) and (87*b*) is similar to inequality (78) in theorem 1. We can note again that the functional dependence of $\mathrm{Re}(\mathcal{S})$ and $\mathrm{Im}(\mathcal{S})$ on $\boldsymbol{P}$ and $\boldsymbol{C}$, respectively, is the same up to a constant factor. Thus, the proof of corollary 1 reduces to the proof of theorem 1 applied independently to $\mathrm{Re}(\mathcal{S})$ and $\mathrm{Im}(\mathcal{S})$.

For this most general setting, it is also possible to formulate the criteria for a solution to the inverse problem to be physical, i.e. to satisfy the conditions $\varepsilon_\perp > 1$, $\varepsilon_\parallel > 1$, $\sigma_\perp > 0$ and $\sigma_\parallel > 0$ (see sections 2.3.4, 2.4.5 and 2.5.3 for particular cases). The resulting expressions, however, are cumbersome, and we omit them here.

2.5.5. Discussion of lossy materials. Altogether, the case of anisotropic permittivity and conductivity has eight independent material parameters and may provide up to eight degrees of freedom to the scattering matrix. If the hypothesis of corollary 1 holds, then the material parameters can be successfully reconstructed from the observables. At the same time, the

particular cases of isotropic conductivity considered in sections 2.5.2 and 2.5.3 illustrate that the introduction of a new physical effect that modifies the scattering mechanism does not necessarily lead to an increased number of the degrees of freedom. Some other simplifications may also reduce the number of degrees of freedom. For example, the assumption that the dielectric axis coincides with the conductivity axis will reduce the number of independent parameters from 8 to 6.

Similarly to sections 1.2 and 2.3.2, the first Born approximation does not provide a physically viable solution in the material, which in the case of a finite conductivity would be a spatially decaying wave. Indeed, in order for the transmitted wave to decay as $z \to +\infty$, the component of its wavenumber normal to the interface should have an imaginary part. However, after the linearization, see equations (26) and (28), the only possible representation for the scattered field is given by (33), where the value of q is always real and is defined by the incident field. Thus, the effect of conductivity is restricted to the changes in the amplitude and phase of the reflected wave.

Let us also recall that even though the observed scattering matrix (15) or (86) has four complex-valued entries, in practice it may appear impossible to distinguish between the relative phase and the common phase that accounts for the travel distance. Hence, it is customary to keep the HH entry of the scattering matrix real, see the discussion around equations (16), which reduces the number of degrees of freedom to 7.

3. Convolution with the fundamental solution and surface potentials

Having discussed the linearized scattering off a half-space filled with various types of materials, we recall that in the context of SAR imaging, the ground reflectivity function is taken in the form of a single layer, see formula (12), or in other words, the target material is considered concentrated only on the surface of the half-space. In this section, we show that for every material considered in section 2, scattering off a material subspace can be equivalently reformulated as scattering off a layer of monopoles on its surface.

3.1. Lossless isotropic target

Let us return for the moment to the simplest case of a perfect isotropic dielectric. We will provide a somewhat different interpretation of the solutions obtained in section 2.3 that will help us justify the use of the ground reflectivity function for SAR imaging in the form of a single layer on the interface $z = 0$; see formula (12).

For the operator $\hat{L}$ of (28), we first define its fundamental solution $\mathcal{E} = \mathcal{E}(z)$ as a solution to the inhomogeneous equation $\hat{L}\mathcal{E} = \delta(z)$ subject to the radiation conditions (29). The fundamental solution exists, is unique, and is given by

$$\mathcal{E}(z) = \frac{1}{2\mathrm{i}q}\,\mathrm{e}^{\mathrm{i}q|z|}. \tag{88}$$

Recall that for the scattering solution in the form (33), we have $B = C$ (see (35)) for the 'homogeneous' part of the solution, $u^{(\mathrm{h})}(z)$; see (30). Consequently, $u^{(\mathrm{h})}(z)$ can be represented in the form of a single-layer potential:

$$u^{(\mathrm{h})}(z) = \mathcal{E}(z) * N\delta(z) = N\mathcal{E}(z). \tag{89}$$

The magnitude of the δ-function at the interface, i.e. the density N of the potential, is equal to the jump of its derivative at $z = 0$, i.e.

$$N = \left[\frac{\mathrm{d}u^{(\mathrm{h})}}{\mathrm{d}z}\right]_{z=0} = 2\mathrm{i}qCu_0, \tag{90}$$

where we use the notation

$$\left[\frac{\mathrm{d}u}{\mathrm{d}z}\right]_{z=0} \stackrel{\text{def}}{=} \left.\frac{\mathrm{d}u}{\mathrm{d}z}\right|_{(M)} - \left.\frac{\mathrm{d}u}{\mathrm{d}z}\right|_{(F)}. \tag{91}$$

The quantity N in (90) depends on the polarization. For the horizontal polarization, the continuity of $\frac{\mathrm{d}u^{(\mathrm{sc})}}{\mathrm{d}z}$ at $z = 0$, see (38), implies that the jump of $\frac{\mathrm{d}u^{(\mathrm{h})}}{\mathrm{d}z}$ should be negative of $\frac{\mathrm{d}u^{(\mathrm{p})}}{\mathrm{d}z}$:

$$\left[\frac{\mathrm{d}u^{(\mathrm{h})}}{\mathrm{d}z}\right]_{z=0} = -\left[\frac{\mathrm{d}u^{(\mathrm{p})}}{\mathrm{d}z}\right]_{z=0},$$

Using (32), we obtain (cf formula (39))

$$N_{\mathrm{HH}} = -\frac{\mathrm{i}q}{2}\frac{k^2}{q^2}(\varepsilon - 1)u_0, \tag{92}$$

where u_0 is the amplitude of the incident wave for the horizontal polarization, i.e. $E^{(\mathrm{inc})}_{0y}$.

For the vertical polarization, formula (44) yields

$$\left[\frac{\mathrm{d}u^{(\mathrm{h})}}{\mathrm{d}z}\right]_{z=0} = -\left[\frac{\mathrm{d}u^{(\mathrm{p})}}{\mathrm{d}z}\right]_{z=0} + (\varepsilon - 1)\left.\frac{\mathrm{d}u^{(\mathrm{inc})}}{\mathrm{d}z}\right|_{z=0},$$

where $u^{(\mathrm{inc})}$ is given by (25*b*). Consequently (cf formula (45)),

$$N_{\mathrm{VV}} = -\frac{\mathrm{i}q}{2}\frac{k^2}{q^2}(\varepsilon - 1)u_0 + \mathrm{i}q(\varepsilon - 1)u_0 = QN_{\mathrm{HH}}. \tag{93}$$

Here, u_0 is the amplitude of the incident wave for the vertical polarization, i.e. $H^{(\mathrm{inc})}_{0y}$.

In either case, (92) or (93), the solution $u^{(\mathrm{h})}(z)$ of (89) coincides in the vacuum region $z < 0$ with the overall scattering solution $u^{(\mathrm{sc})}(z)$; see formulae (33) and (30). This means that the reflected field given by the first Born approximation for the scattering off a material half-space can be equivalently represented as the reflected field due to the linearized scattering off a specially chosen δ-layer at the boundary of the half-space. Moreover, for both horizontal and vertical polarizations, the magnitude of the single layer is proportional to $(\varepsilon - 1)u_0$ or equivalently, to the scalar lossless ground reflectivity function (7) times the incident field at the interface:

$$N \propto (\varepsilon - 1)u_0 = \left(\frac{c^2}{v^2} - 1\right)u_0 = c^2 v u_0.$$

This explains why for the analysis of the reflected field in the framework of the first Born approximation, the ground reflectivity function can be chosen in the form of a single layer at the material interface; see formula (12). We also note that according to the electromagnetic equivalence theorem by Schelkunoff [24], the field on a given region, regardless of its actual sources located outside of this region, can be reproduced as the field from the specially chosen auxiliary sources at the boundary of the region.

Given representation (89) of the reflected field as a convolution with the fundamental solution, one can formulate a natural question of whether or not the entire scattering solution can be obtained as a convolution integral. In fact, equation (28) has been solved by convolution in [5]. This approach, however, suffers from two limitations. First, the convolution of the fundamental solution (88) with the right-hand side $g(z)$ of (28) leads to a diverging improper integral over the interval $0 \leqslant z < \infty$, and the use of the limiting absorption principle in [5] for 'fixing' the divergence lacks mathematical rigor. But even disregarding that, the second limitation is more important. For a bounded continuous right-hand side $g(z)$ in (28), the convolution integral yields a C^1 smooth function. This implies, in particular, the continuity of the resulting solution and its first derivative at $z = 0$, which corresponds to the horizontal polarization only. In other words, a straightforward convolution-based approach cannot account

for any boundary conditions other than (38) and hence cannot be used for studying other polarizations. To analyze the vertical polarization, an additional singular term at $z = 0$ due to boundary condition (44) should be taken into account along with the right-hand side $g(z)$.

3.2. Anisotropic and lossy targets

The approach of section 3.1 can be extended to include more complex cases considered in table 2. The new effects to be described are the cross-polarized components in the scattered field and the phase shift due to a finite conductivity.

For an incident wave in one of the two basic polarizations, the presence of two components in the scattered field (co-polarized and cross-polarized) can be described by a two-dimensional vector δ-layer. In doing so, formula (89) applies to each component of the vector δ-layer separately. For a birefringent scatterer considered in section 2.4, we can use relation (90) and express the components of the vector density using reflection coefficients defined by formulae (73):

$$\boldsymbol{M}_{\mathrm{H}} = \begin{bmatrix} N_{\mathrm{HH}} \\ N_{\mathrm{VH}} \end{bmatrix} = 2\mathrm{i}qE_{0y}^{(\mathrm{inc})} \begin{bmatrix} S_{\mathrm{HH}} \\ S_{\mathrm{VH}} \end{bmatrix}, \quad \boldsymbol{M}_{\mathrm{V}} = \begin{bmatrix} N_{\mathrm{VV}} \\ N_{\mathrm{HV}} \end{bmatrix} = 2\mathrm{i}qH_{0y}^{(\mathrm{inc})} \begin{bmatrix} S_{\mathrm{VV}} \\ S_{\mathrm{HV}} \end{bmatrix}. \tag{94}$$

A finite conductivity affects the density of the δ-layers given by formulae (92)–(94) through the modified dielectric tensor $\tilde{\boldsymbol{\varepsilon}}$ of (81) and the corresponding changes in the reflection coefficients (see section 2.5.1).

4. Application to polarimetric target decomposition

The polarimetric target decomposition [14, 25] can be viewed as a heuristic method of solving the inverse scattering problem. Basically, the goal is to represent the scattering matrix[9] as a linear combination of the basis matrices:

$$\mathcal{S} = c_1\mathcal{S}_1 + c_2\mathcal{S}_2 + c_3\mathcal{S}_3 + c_4\mathcal{S}_4, \tag{95}$$

where each of $\mathcal{S}_i$, $i = 1, 2, 3, 4$, represents a particular scattering mechanism, and the c_i, $i = 1, 2, 3, 4$, are complex-valued coefficients to be determined. For example, the Pauli matrices

$$\mathcal{S}_1 = \begin{bmatrix} 1 & 0 \\ 0 & 1 \end{bmatrix}, \quad \mathcal{S}_2 = \begin{bmatrix} 1 & 0 \\ 0 & -1 \end{bmatrix}, \quad \mathcal{S}_3 = \begin{bmatrix} 0 & 1 \\ 1 & 0 \end{bmatrix}, \text{ and } \quad \mathcal{S}_4 = \begin{bmatrix} 0 & -\mathrm{i} \\ \mathrm{i} & 0 \end{bmatrix}$$

may be associated with single-bounce and double-bounce scattering off plane surfaces with different orientation; see [14, chapter 6]. The choice of the basis $\mathcal{S}_i$ for decomposition specifies the range of admissible scattering mechanisms, whereas the decomposition coefficients c_i determine the (relative) weights for individual mechanisms.

If some *a priori* knowledge about the actual scattering process is available, then it may be beneficial to choose one (or more) of the matrices $\mathcal{S}_i$ as the matrix of reflection coefficients for a given scattering mechanism (see, e.g., formula (B.1)). This choice allows one to estimate the role of a particular mechanism in the overall scattering, and makes it easier to interpret the results of decomposition. For example, some foliage penetration and terrain scattering models [25, section VI] involve multiple scattering channels where one of the stages is the 'mirror' reflection from the ground. The models developed in section 2 may be used to represent this 'mirror reflection' stage for sufficiently large radar wavelengths that allow one to neglect the roughness of the surface.

[9] In practice, the decomposition is often applied to the coherency and covariance matrices, whose entries are second-order moments of the particular combinations of entries of the Sinclair scattering matrix; see [14, chapters 3, 6]. The decomposition considered here is called the 'coherent decomposition.'

In the current work, we analyze the Sinclair scattering matrices built from physical principles. We can therefore expect that if an appropriate basis is chosen, then the polarimetric target decomposition will yield the corresponding material characteristics. For a lossless material, the matrix of reflection coefficients (73) can be equivalently represented as

$$\mathcal{S} = \begin{bmatrix} S_{\mathrm{HH}} & S_{\mathrm{HV}} \\ S_{\mathrm{VH}} & S_{\mathrm{VV}} \end{bmatrix} = -\frac{1}{4}\frac{k^2}{q^2}\left((\varepsilon_\perp - 1)\mathcal{S}_1 + \Delta\varepsilon\mathcal{S}_2 + \frac{q}{k}\alpha\beta\Delta\varepsilon\mathcal{S}_3 - \frac{K}{k}\gamma\beta\Delta\varepsilon\mathcal{S}_4\right), \tag{96}$$

where the matrices $\mathcal{S}_i$, $i = 1, 2, 3, 4$, are given by

$$\mathcal{S}_1 = \begin{bmatrix} 1 & 0 \\ 0 & \dfrac{K^2 - q^2}{k^2} \end{bmatrix}, \quad \mathcal{S}_2 = \begin{bmatrix} \beta^2 & 0 \\ 0 & \dfrac{K^2\gamma^2 - q^2\alpha^2}{k^2} \end{bmatrix}, \quad \mathcal{S}_3 = \begin{bmatrix} 0 & 1 \\ -1 & 0 \end{bmatrix} \text{ and } \mathcal{S}_4 = \begin{bmatrix} 0 & 1 \\ 1 & 0 \end{bmatrix}.$$

Hence, we can interpret formula (96) as a polarimetric target decomposition of type (95) with $c_1 = \varepsilon_\perp - 1$, $c_2 = \Delta\varepsilon$, $c_3 = q\alpha\beta\Delta\varepsilon/k$ and $c_4 = -K\gamma\beta\Delta\varepsilon/k$ (up to a common multiplicative factor of $-\frac{1}{4}\frac{k^2}{q^2}$, which can also be combined with the geometric attenuation coefficient). If we have decomposition (96), then of the four material parameters to be reconstructed, the two permittivities are obtained directly from c_1 and c_2, while the relations for c_3 and c_4 provide two equations for two of the three directional cosines of the optical axis (with the third expressed via (49)). The problem however is that the entries of the matrix $\mathcal{S}_2$ depend on the material parameters (direction angles for the optical axis) and cannot be defined without having to solve the inverse problem first. It is possible though to break the loop by taking any diagonal matrix not proportional to $\mathcal{S}_1$ instead of $\mathcal{S}_2$. For example, the following set of matrices

$$\mathcal{S}_1 = \begin{bmatrix} 1 & 0 \\ 0 & \dfrac{K^2 - q^2}{k^2} \end{bmatrix}, \qquad \mathcal{S}_2' = \begin{bmatrix} 0 & 0 \\ 0 & \dfrac{K^2}{k^2} \end{bmatrix} \quad \mathcal{S}_3 = \begin{bmatrix} 0 & -1 \\ 1 & 0 \end{bmatrix} \text{ and } \mathcal{S}_4 = \begin{bmatrix} 0 & 1 \\ 1 & 0 \end{bmatrix} \tag{97}$$

forms a basis in the space of 2×2 matrices with real entries, does not depend on the material properties and hence can be used for target decomposition. The disadvantage of this set is that the resulting value of c_2 will, generally speaking, differ from $\Delta\varepsilon$, and thus the values of ξ, α and γ calculated from c_1, c_3 and c_4 will also be incorrect. Still, expansion (95) with respect to basis (97) is capable of detecting several types of configurations (see figure 1):

(i) isotropy ($\zeta = 0$), by observing that $c_2 = c_3 = c_4 = 0$;
(ii) the optical axis being either parallel to the incidence plane ($\beta = 0$) or perpendicular to it ($\beta = 1$, $\alpha = \gamma = 0$), when $c_2 \neq 0$, $c_3 = c_4 = 0$;
(iii) the optical axis being horizontal, excluding the cases in item (ii) ($\alpha \neq 0$, $\beta \neq 0$, $\gamma = 0$) when $c_3 \neq 0$, $c_4 = 0$;
(iv) the optical axis lying in the plane normal to both the interface and the incidence plane, excluding the cases in item (ii) ($\alpha = 0$, $\beta \neq 0$, $\gamma \neq 0$) when $c_3 = 0$, $c_4 \neq 0$;
(v) any of the 'main diagonal' directions of the optical axis ($|\alpha| = |\beta| = |\gamma| = 1/\sqrt{3}$), when $c_2 = 0$, $c_3 \neq 0$, $c_4 \neq 0$, etc.

Thus, basis (97) appears suitable for the *qualitative classification* of birefringent targets, although exact determination of the material parameters still requires solving a nonlinear system (73) that consists of four equations. It is to be noted though that in practice, the equalities in criteria (i)–(v) shall be replaced by thresholds that would take into account the accuracy of the measurements and the noise levels. The questions related to noise and experimental accuracy will be addressed in a future publication.

Lossy targets can be identified by detecting a phase shift other than 0 or π between the channels. As the imaginary part of the matrix $\mathcal{S}$ is similar in structure to the real part (see formula (86)), a complex counterpart of the set of matrices (97) can be used for the decomposition of $\mathrm{Im}(\mathcal{S})$, which is equivalent to allowing the coefficients c_i to become complex.

5. Discussion and future work

We have analyzed the linearized scattering of a plane transverse electromagnetic wave off a material half-space filled with an anisotropic (birefringent) weakly conductive dielectric. Our main findings are as follows.

- We have shown that the first Born approximation correctly predicts the scattered field (both amplitude and phase for each polarization) in the vacuum region.
- We have demonstrated that with the polarization and anisotropy taken into account, the linearized scattering off a material half-space can still be equivalently reformulated in the vacuum region as scattering off a specially chosen δ-layer at the interface. This justifies the choice of a ground reflectivity function in the form of a single layer at the surface of a target, which is common for SAR applications.
- The corresponding inverse scattering problem consists in reconstructing the material characteristics, i.e. the permittivities, conductivities and direction angles at the target, from the observable quantities, i.e. from the four complex-valued entries of the Sinclair scattering matrix. We have provided a necessary and sufficient condition (see theorem 1 and corollary 1) for this inverse problem to have a solution in the linearized framework.

As of yet, our analysis is limited to 'mirror' scattering off a flat surface, and does not account for backscattering. Hence, in the context of SAR, it may be useful for bistatic rather than monostatic imaging, i.e. for the case when the transmitting and receiving antennas are two different antennas at two different locations. Another possible application of this 'mirror reflection' mechanism is to be a ground reflection component in composite foliage penetration and terrain scattering models [25, section VI].

To account for backscattering, one needs to include additional scattering mechanisms, e.g., surface roughness and/or variation of material parameters on the scale of the wavelength. This will be a subject for the future study.

In this paper, we have not formally considered any variation of material characteristics along the interface; that is why we could assume that all the waves have a common horizontal component K of the wavenumber; see figure 1. It is obvious, however, that our analysis extends with no change to the case of slowly varying material characteristics. This means, in particular, that we can consider ground reflectivity functions that vary along the interface, but only if $\lambda \ll d$, where λ is the wavelength and d is the characteristic scale of material variations defined, e.g., as $d^{-1} \sim |\nabla\hat{\varepsilon}|/|\hat{\varepsilon}|$, where $\hat{\varepsilon}$ can stand for any of the actual physical quantities that we have taken into account. The constraint $\lambda \ll d$ should not present a major limitation for SAR applications, because the SAR resolution is typically much larger than the wavelength anyway (see [8]). On the other hand, our current analysis does not apply to short-scale material variations, $d \sim \mathcal{O}(\lambda)$, and to include those it will need to be modified. This is related to accounting for backscattering.

Our motivation for analyzing the first Born approximation in the case of polarized waves and anisotropic targets was the possibility of building a polarimetric SAR ambiguity theory similarly to how it is done in the scalar case. This, in particular, may help extend the results of [26] on mitigating the ionospheric distortions of spaceborne SAR images from the case of scalar imaging to the case of polarimetric imaging that also involves Faraday rotation in the magnetized ionosphere. It may also appear useful for miSAR applications (see section 4). Based on the analysis in this paper, we conclude that the polarimetric ambiguity theory can be built provided that the hypotheses of theorem 1 and corollary 1 hold. It is also to be noted that the limitation of solvability of the linearized inverse problem imposed by theorem 1 is apparently due to the type of the material that we have chosen (a birefringent dielectric with

weak anisotropic conductivity) rather than to the linearization itself (see appendix C). Giving a physical interpretation to inequality (78), as well as, perhaps, considering other materials and answering a related question of having non-physical solutions to the inverse problem, see sections 2.3.4, 2.4.5, 2.5.3 and 2.5.4, will be a subject for the future study.

Acknowledgments

This work was supported by the US Air Force Office of Scientific Research (AFOSR) under agreement FA9550-10-1-0092. We would like to thank two anonymous referees for their helpful comments.

Appendix A. Governing equations

By subtracting equations (4) from respective equations (1) and using (3), we obtain the following governing equations for the scattered fields:

$$\begin{aligned}&\frac{1}{c}\frac{\partial \boldsymbol{H}^{(\mathrm{sc})}}{\partial t}+\nabla\times\boldsymbol{E}^{(\mathrm{sc})}=\boldsymbol{0},\quad \nabla\cdot\boldsymbol{H}^{(\mathrm{sc})}=0,\\ &\frac{1}{c}\frac{\partial \boldsymbol{E}^{(\mathrm{sc})}}{\partial t}-\nabla\times\boldsymbol{H}^{(\mathrm{sc})}=-\frac{1}{c}\left[(\boldsymbol{\varepsilon}-\mathcal{I})\cdot\frac{\partial \boldsymbol{E}}{\partial t}+4\pi\boldsymbol{\sigma}\cdot\boldsymbol{E}\right],\quad \nabla\cdot\boldsymbol{E}^{(\mathrm{sc})}=-\nabla\cdot(\boldsymbol{D}-\boldsymbol{E}).\end{aligned}\tag{A.1}$$

Note that the scattered field $\boldsymbol{E}^{(\mathrm{sc})}$ appears both on the left-hand side and on the right-hand side of the second pair of equations of (A.1). Differentiating the Ampère law in (A.1) with respect to time, we have

$$\frac{1}{c}\frac{\partial^2 \boldsymbol{E}^{(\mathrm{sc})}}{\partial t^2}-\frac{\partial}{\partial t}\nabla\times\boldsymbol{H}^{(\mathrm{sc})}=-\frac{1}{c}\left[(\boldsymbol{\varepsilon}-\mathcal{I})\cdot\frac{\partial^2 \boldsymbol{E}}{\partial t^2}+4\pi\boldsymbol{\sigma}\cdot\frac{\partial \boldsymbol{E}}{\partial t}\right],\tag{A.2}$$

and taking the curl (i.e. $\nabla\times$) of the Faraday law in (A.1), we obtain

$$\frac{1}{c}\frac{\partial}{\partial t}\nabla\times\boldsymbol{H}^{(\mathrm{sc})}+\nabla\times\nabla\times\boldsymbol{E}^{(\mathrm{sc})}=\frac{1}{c}\frac{\partial}{\partial t}\nabla\times\boldsymbol{H}^{(\mathrm{sc})}-\Delta\boldsymbol{E}^{(\mathrm{sc})}+\nabla\nabla\cdot\boldsymbol{E}^{(\mathrm{sc})}=\boldsymbol{0}.\tag{A.3}$$

The operation $\nabla\nabla\cdot$ on the right-hand side of equation (A.3), see also (A.4) and (A.6), means the gradient of the divergence of the corresponding vector. Substituting the time derivative of $\nabla\times\boldsymbol{H}^{(\mathrm{sc})}$ from equation (A.3) into equation (A.2), and also taking into account the Gauss law of electricity in (A.1), we arrive at

$$\frac{1}{c^2}\frac{\partial^2 \boldsymbol{E}^{(\mathrm{sc})}}{\partial t^2}-\Delta\boldsymbol{E}^{(\mathrm{sc})}=-\frac{\boldsymbol{\varepsilon}-\mathcal{I}}{c^2}\cdot\frac{\partial^2 \boldsymbol{E}}{\partial t^2}-\frac{4\pi\boldsymbol{\sigma}}{c^2}\cdot\frac{\partial \boldsymbol{E}}{\partial t}+\nabla\nabla\cdot(\boldsymbol{D}-\boldsymbol{E}),\tag{A.4}$$

where on the left-hand side we have the standard constant coefficient d'Alembert operator acting on $\boldsymbol{E}^{(\mathrm{sc})}$, and on the right-hand side we have additional occurrences of the scattered field via equations (2) and (5). Similarly, the incident electric field that provides the source terms for (A.4) is governed by the d'Alembert equation

$$\frac{1}{c^2}\frac{\partial^2 \boldsymbol{E}^{(\mathrm{inc})}}{\partial t^2}-\Delta\boldsymbol{E}^{(\mathrm{inc})}=-\frac{4\pi}{c^2}\frac{\partial \boldsymbol{j}^{(\mathrm{ex})}}{\partial t}.\tag{A.5}$$

If the target material is isotropic, i.e. if $\boldsymbol{\varepsilon}=\frac{c^2}{v^2}\mathcal{I}$, where $v=v(\boldsymbol{x})$ is the local propagation speed, and $\boldsymbol{\sigma}=\sigma\mathcal{I}$, then equation (A.4) simplifies, and we have

$$\frac{1}{c^2}\frac{\partial^2 \boldsymbol{E}^{(\mathrm{sc})}}{\partial t^2}-\Delta\boldsymbol{E}^{(\mathrm{sc})}=v(\boldsymbol{x})\frac{\partial^2 \boldsymbol{E}}{\partial t^2}-\frac{4\pi\sigma}{c^2}\frac{\partial \boldsymbol{E}}{\partial t}+\nabla\nabla\cdot\left(\frac{c^2}{v^2}-1\right)\boldsymbol{E},\tag{A.6}$$

where the scalar quantity

$$\nu(\boldsymbol{x}) \stackrel{\text{def}}{=} \frac{1}{c^2} - \frac{1}{v(\boldsymbol{x})^2} \tag{A.7}$$

is known as the (target) reflectivity function (see, e.g., [4, chapter 6]).

In the context of inverse scattering, equation (A.6) shall be interpreted as an equation for ν and σ, whereas $\boldsymbol{E}^{(\mathrm{sc})}$ provides the data. A key difficulty, however, is that the scattered field is not known at the target. For example, for the synthetic aperture radar (SAR) applications, see, e.g., [4], $\boldsymbol{E}^{(\mathrm{sc})}$ is known at the receiving antenna, which is airborne or spaceborne, whereas at the target, i.e. on the ground, it is not known. This makes the inverse problem nonlinear, because the unknown material characteristics ν and σ are multiplied on the right-hand side of (A.6) with the unknown scattered field.

A well-known remedy is to assume that the scattering is weak, and employ the first Born approximation; see [3, chapter XIII]. Under this assumption, the total field $\boldsymbol{E}$ on the right-hand side of equation (A.6) is replaced with the incident field $\boldsymbol{E}^{(\mathrm{inc})}$ only, which makes the inverse problem linear. The rationale is that in the case of weak scattering, both the deviations of the material parameters from the vacuum values are small, and the scattered field $\boldsymbol{E}^{(\mathrm{sc})}$ is also small, so their products on the right-hand side of equation (A.6) can be neglected. Moreover, the last term on the right-hand side of (A.6) drops as well because we first invoke the Gauss law of electricity from the system (1) in the form $\nabla \cdot \frac{c^2}{v^2}\boldsymbol{E} = 0$ and then the Gauss law of electricity for the incident field from the system (4). Altogether this yields

$$\frac{1}{c^2}\frac{\partial^2 \boldsymbol{E}^{(\mathrm{sc})}}{\partial t^2} - \Delta \boldsymbol{E}^{(\mathrm{sc})} = \nu \frac{\partial^2 \boldsymbol{E}^{(\mathrm{inc})}}{\partial t^2} - \frac{4\pi\sigma}{c^2}\frac{\partial \boldsymbol{E}^{(\mathrm{inc})}}{\partial t}. \tag{A.8}$$

The first Born approximation can also be given another equivalent interpretation based on the perturbation theory. In this framework, the zeroth-order solution is the incident field governed by equation (A.5), and the equation for the first-order perturbation is obtained from equation (A.6) by replacing the total solution on its right-hand side by the zeroth-order solution, which yields equation (A.8). Again, considering no more than first-order perturbations is justified only if the scattering is weak, i.e. if $|\nu| \ll 1/c^2$ and $\sigma/\omega \ll 1$, where ω is the typical frequency. These two requirements are equivalent to treating the difference between the complex electric permittivity and one as a small parameter; it is used for deriving the first Born approximation for a hierarchy of scattering problems in section 2 (see formulae (22) and (25)).

Appendix B. Proof of theorem 1

Reflection coefficients obtained with the help of the first Born approximation for a lossless birefringent target are given by formulae (73). Introducing the new variable $\xi = \varepsilon_\perp - 1$ and denoting $\zeta = \Delta\varepsilon$, we rewrite these formulae as follows:

$$\begin{aligned}
S_{\mathrm{HH}} &= -\frac{1}{4}\frac{k^2}{q^2}(\xi + \beta^2\zeta),\\
S_{\mathrm{VV}} &= \frac{1}{4}\left((\xi + \alpha^2\zeta) - \frac{K^2}{q^2}(\xi + \gamma^2\zeta)\right),\\
S_{\mathrm{HV}} &= -\frac{1}{4}\frac{k}{q}\left(\alpha - \frac{K}{q}\gamma\right)\zeta\beta,\\
S_{\mathrm{VH}} &= \frac{1}{4}\frac{k}{q}\left(\alpha + \frac{K}{q}\gamma\right)\zeta\beta.
\end{aligned} \tag{B.1}$$

These expressions can also be obtained by linearization of the exact reflection coefficients given in [22]; for a special case of $\gamma = 0$, formulae (B.1) can be obtained by linearization of the results of [23] as well.

Formulae (B.1) define four functions of the arguments ξ, ζ, α and γ (with β expressed via (49)). Therefore, we can introduce the Jacobian

$$\left|\frac{\partial(S_{\mathrm{HH}}, S_{\mathrm{VV}}, S_{\mathrm{HV}}, S_{\mathrm{VH}})}{\partial(\xi, \zeta, \alpha, \gamma)}\right| = \left|\frac{Kk^4(K^2(\alpha^2-1) - q^2(\gamma^2-1))\zeta^2}{128q^7}\right|. \tag{B.2}$$

One can see that the right-hand side of (B.2) is nonzero at least for some values of the arguments. Indeed, if $\zeta \neq 0$ (i.e. if the material is anisotropic), then we can choose independent directional cosines α and γ so that the numerator on the right-hand side of (B.2) is nonzero. Thus, in the vicinity of such points in the parameter space, the transformation from $(\xi, \zeta, \alpha, \gamma)$ to $(S_{\mathrm{HH}}, S_{\mathrm{VV}}, S_{\mathrm{HV}}, S_{\mathrm{VH}})$ is locally non-degenerate, and preserves the number of degrees of freedom. This local non-degeneracy, however, does not guarantee that the system (B.1) can be resolved for $(\xi, \zeta, \alpha, \gamma)$ given arbitrary scattering data (i.e. the left-hand side of the system (B.1)).

To find out when the system (B.1) has a solution, we denote $Z = K/q = \tan\theta_i$, and transform the last two equations of the system to

$$S^+ = \gamma\zeta\beta, \quad S^- = \alpha\zeta\beta, \tag{B.3}$$

where

$$S^+ = \frac{2}{Z\sqrt{1+Z^2}}(S_{\mathrm{VH}} + S_{\mathrm{HV}}) \quad \text{and} \quad S^- = \frac{2}{\sqrt{1+Z^2}}(S_{\mathrm{VH}} - S_{\mathrm{HV}}).$$

Next, we introduce

$$D = \frac{S^-}{S^+} = \frac{\alpha}{\gamma}, \tag{B.4}$$

which, together with (49), yields

$$\beta^2 = 1 - \gamma^2(1+D^2). \tag{B.5}$$

We can eliminate ξ from the first two equations of (B.1) to obtain

$$\tilde{S} = \zeta W, \tag{B.6}$$

where

$$\begin{aligned} \tilde{S} &= 4\left(S_{\mathrm{VV}} + S_{\mathrm{HH}}\frac{1-Z^2}{1+Z^2}\right), \\ W &= (Z^2-1) + \gamma^2(D^2 - Z^2 + (1-Z^2)(1+D^2)). \end{aligned} \tag{B.7}$$

Using equations (B.5), (B.6) and the second equation of (B.3), we arrive at

$$P^2\gamma^2D^2\big(1-\gamma^2(1+D^2)\big) = W^2, \tag{B.8}$$

where $P = \tilde{S}/S^-$. As W in formula (B.7) is linear w.r.t. γ^2, equation (B.8) is biquadratic w.r.t. γ. A solution for γ^2 exists if and only if the corresponding discriminant is nonnegative, which can be shown to be equivalent to

$$P^2 \geqslant 4\frac{(D^2-Z^2)(Z^2-1)}{D^2}. \tag{B.9}$$

Condition (B.9) can be transformed into (78) using equations (B.3), (B.7) and (B.8).

It should also be noted that whereas the right-hand side of (B.8) is always nonnegative, the left-hand side is nonnegative only if

$$0 \leqslant \gamma^2 \leqslant \frac{1}{1+D^2}. \tag{B.10}$$

This means that if condition (B.9) for the existence of a solution to (B.8) with respect to γ^2 is satisfied, then this solution, i.e. γ^2, satisfies (B.10). If (B.9) has two solutions, then both should satisfy (B.10). The second inequality in (B.10), together with equations (B.4) and (B.5), also ensures that $0 \leqslant \alpha^2 \leqslant 1$ and $0 \leqslant \beta^2 \leqslant 1$ (see (49)).

If condition (B.9) (or its equivalent (78)) is satisfied, then γ^2 can be found by solving (B.8), and the sign of γ can be chosen arbitrarily because the system (B.1) is invariant w.r.t. the transformation $(\alpha, \beta, \gamma) \longrightarrow (-\alpha, -\beta, -\gamma)$. Then, the value of α is obtained from (B.4), ζ from (B.6), β from any of the equations (B.3) and ξ from the first equation of system (B.1). With that, all the material parameters are determined, which completes the proof of theorem 1.

Appendix C. Numerical study of the exact formulation

Theorem 1 indicates that the linearized inverse problem has a solution only for certain combinations of the reflection coefficients S_{HH}, S_{VV}, S_{HV}, S_{VH} and the incidence angle θ_i. For example, if $\alpha = 0$, then $S_{\mathrm{HV}} = S_{\mathrm{VH}}$, see formulae (B.1), and the right-hand side of inequality (78) is negative provided that $\theta_i > \pi/4$. Hence, inequality (78) holds automatically, and the linearized inverse problem always has a solution for $\theta_i > \pi/4$. On the other hand, for $\theta_i < \pi/4$ inequality (78) puts an additional constraint on the values of the reflection coefficients and thus implies a limitation of solvability of the linearized inverse problem.

While inequality (78) may be given a physical interpretation later on, currently we would like to try and answer the question of whether the foregoing limitation of solvability (theorem 1) is due to the type of the target material that we have chosen (a birefringent dielectric with weak anisotropic conductivity) or to the linearization itself. Expressions for the exact (i.e. not linearized) reflection coefficients can be found, e.g., in [22, equation (6.61)]. However, that system (unlike the linearized system (B.1)) has proven too complicated for analytical inversion. Instead, we employ a numerical approach. First, we sample the domain of feasible material parameters (typically, $\varepsilon_{\|}$ and $\varepsilon_{\perp}$ are taken between 1 and 5) with a sufficiently high rate, and calculate the exact reflection coefficients for every sample, i.e. solve the direct problem exactly with the help of [22]. In doing so, we obtain a cloud of points in the three-dimensional space of coefficients S_{HH}, S_{VV} and $S_{\mathrm{HV}} = S_{\mathrm{VH}}$. Areas of no solution would correspond to the regions with no points inside the cloud, i.e. to the voids. To see whether or not there are any voids, we plot several cross-sections of the cloud normal to the S_{VH} axis. As, however, the cloud consists of discrete points, we rather take slices of finite thickness in S_{VH} and collapse all the points inside each slice onto the $(S_{\mathrm{HH}}, S_{\mathrm{VV}})$ plane for plotting.

The visualization we have described reveals distinct voids in the cloud of the results for the exact formulation of the direct scattering problem. Those voids can, in particular, be clearly seen in figure C1, where we show the values of $\varepsilon_{\|}$ as they depend on S_{HH}, S_{VV} and S_{VH}. Inside the voids, the solution to the original (i.e. not linearized) inverse problem does not exist, because the corresponding values of the reflection coefficients cannot be obtained using any choice of the material parameters.

Moreover, as $\theta_i = 2\pi/9 \leqslant \pi/4$ in figure C1, the linearized problem may have no solution according to theorem 1. The region where the linearized solution does not exist (see inequality (78)) is bounded by two straight red lines on each of the plots in figure C1. We see that when the scattering is weak, i.e. when all the reflection coefficients S_{HH}, S_{VV} and S_{VH} are small, those red lines appear tangential to the apparent boundaries of a given void that corresponds to the exact formulation. This is precisely the behavior that would be natural to expect in the case when both the linearized and the original inverse problem have regions with no solution.

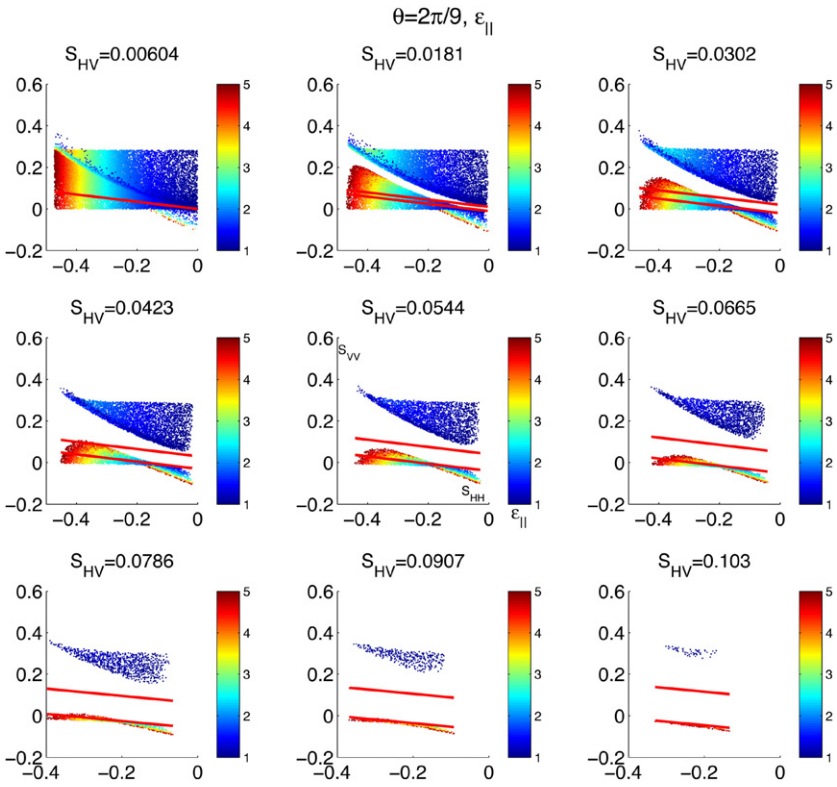

Figure C1. $\varepsilon_\parallel$ as a function of the exact reflection coefficients for $\alpha = 0$ and $\theta_i = 2\pi/9$. The value of $\varepsilon_\parallel$ is indicated by color. The horizontal axis is $S_{\rm HH}$ and the vertical axis is $S_{\rm VV}$, as indicated in the middle plot. The approximate ranges for the cloud of the results are $-0.5 \leqslant S_{\rm HH} \leqslant 0$, $-0.2 \leqslant S_{\rm VV} \leqslant 0.6$ and $0 \leqslant |S_{\rm VH}| \leqslant 0.11$. The gap between the two red lines corresponds to the region for which inequality (78) does not hold, i.e. for which the linearized inverse problem has no solution.

This tangential behavior can be observed more clearly in figure C2, which is a zoom-in of the middle plot in the top row of figure C1.

Let us also note that whereas for larger values of the incidence angle, $\theta_i > \pi/4$, the linearized inverse problem has a solution, the original, i.e. not linearized, inverse problem may still have no solutions. We illustrate that in figure C3, which is similar to figure C1 in every respect except that $\theta_i = \pi/3$ and the computed ranges for $S_{\rm HH}$, $S_{\rm VV}$ and $S_{\rm VH}$ appear somewhat different. From figure C3, it is apparent that when all three coefficients $S_{\rm HH}$, $S_{\rm VV}$ and $S_{\rm VH}$ are small, which is basically equivalent to the linear regime (weak scattering), there are no voids in the cloud of the results and the solution exists, as expected. As, however, the scattering becomes stronger so that $S_{\rm VH}$ increases, a void appears again indicating a limitation of solvability[10].

Altogether, our rigorous analysis of the first Born approximation along with the simulations conducted for the unabridged formulation indicates that for the weak scattering regime when the two formulations are supposed to be close, the linear and nonlinear problems indeed have or do not have a solution simultaneously. In particular, the full nonlinear problem will have no solution for the same combinations of parameters for which the linearized problem

[10] The voids we discuss here provide additional constraints, beyond the general limitations on the solvability of the inverse problem that come, e.g., from the conservation of energy.

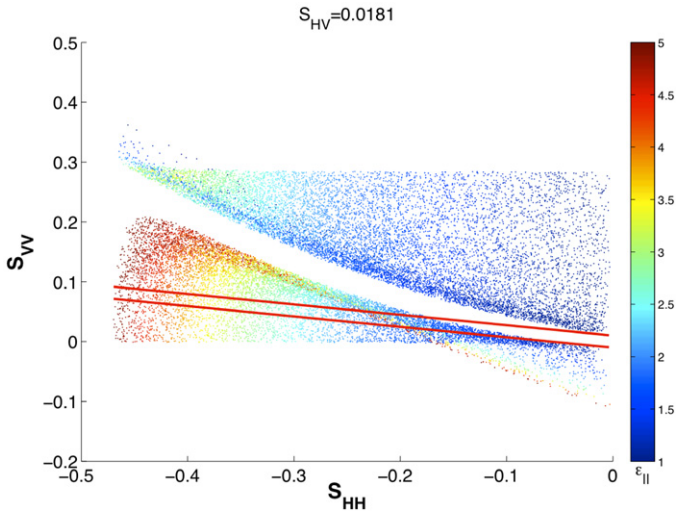

Figure C2. Zoom-in of the middle plot in the top row of figure C1.

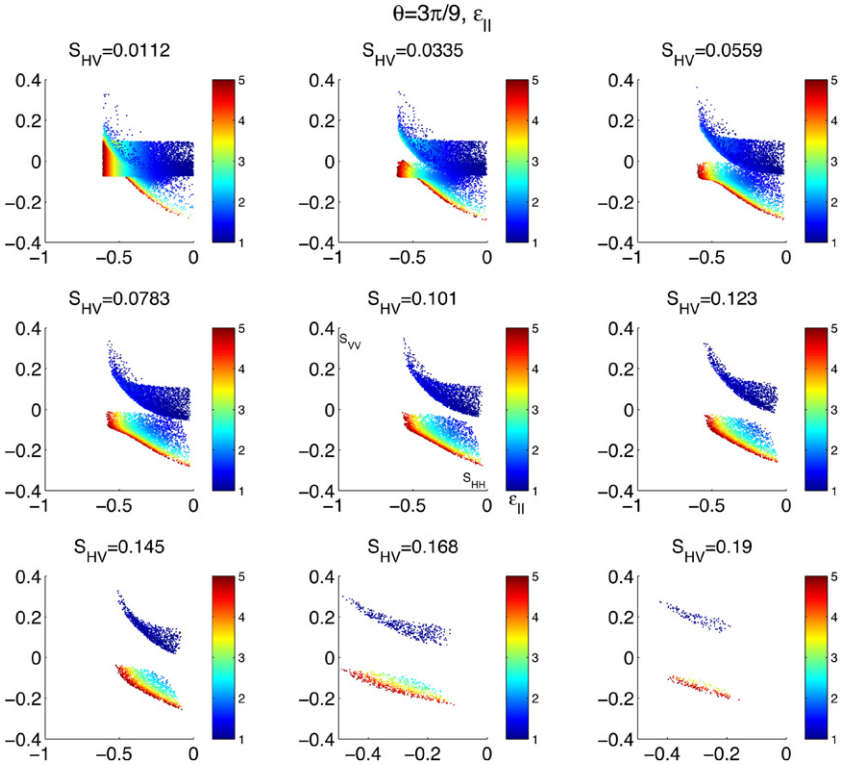

Figure C3. $\varepsilon_{\|}$ as a function of the exact reflection coefficients for $\alpha = 0$ and $\theta_i = \pi/3$. The value of $\varepsilon_{\|}$ is indicated by color. The horizontal axis is S_{HH} and the vertical axis is S_{VV}, as indicated in the middle plot. The approximate ranges for the cloud of the results are $-1 \leqslant S_{\mathrm{HH}} \leqslant 0$, $-0.4 \leqslant S_{\mathrm{VV}} \leqslant 0.4$ and $0 \leqslant |S_{\mathrm{VH}}| \leqslant 0.2$.

has no solution. This means that the linearization is apparently not the reason for the loss of solvability, and that the result of theorem 1 should most likely be attributed to the properties of the target material that we have taken for our analysis rather than 'blamed' on the first Born approximation.

References

[1] Landau L D and Lifshitz E M 1975 *Course of Theoretical Physics: Vol 2. The Classical Theory of Fields* 4th edn (Oxford: Pergamon) (translated from the Russian edition by Morton Hamermesh)

[2] Landau L D and Lifshitz E M 1984 *Course of Theoretical Physics: Vol 8. Electrodynamics of Continuous Media (Pergamon International Library of Science, Technology, Engineering and Social Studies)* (Oxford: Pergamon) (translated from the 2nd Russian edition by J B Sykes, J S Bell and M J Kearsley; 2nd Russian edition revised by E M Lifshitz and L P Pitaevskii)

[3] Born M and Wolf E 1999 *Principles of Optics: Electromagnetic Theory of Propagation, Interference and Diffraction of Light* 7th (expanded) edn, contributions by A B Bhatia, P C Clemmow, D Gabor, A R Stokes, A M Taylor, P A Wayman and W L Wilcock (Cambridge: Cambridge University Press)

[4] Cheney M and Borden B 2009 *Fundamentals of Radar Imaging* (*CBMS-NSF Regional Conference Series in Applied Mathematics* vol 79) (Philadelphia: SIAM)

[5] Oristaglio M L 1985 Accuracy of the Born and Rytov approximations for reflection and refraction at a plane interface *J. Opt. Soc. Am.* A **2** 1987–93

[6] Lin F C and Fiddy M A 1992 The Born–Rytov controversy: I. Comparing analytical and approximate expressions for the one-dimensional deterministic case *J. Opt. Soc. Am.* A **9** 1102–10

[7] Marks D L 2006 A family of approximations spanning the Born and Rytov scattering series *Opt. Express* **14** 8837–48

[8] Cheney M 2001 A mathematical tutorial on synthetic aperture radar *SIAM Rev.* **43** 301–12 (electronic)

[9] Cheney M and Nolan C J 2004 Synthetic-aperture imaging through a dispersive layer *Inverse Problems* **20** 507–32

[10] Nolan C J and Cheney M 2004 Microlocal analysis of synthetic aperture radar imaging *J. Fourier Anal. Appl.* **10** 133–48

[11] Cheney M and Borden B 2008 Imaging moving targets from scattered waves *Inverse Problems* **24** 035005

[12] Franceschetti G and Lanari R 1999 *Synthetic Aperture Radar Processing (Electronic Engineering Systems Series)* (Boca Raton, FL: CRC Press)

[13] Mott H 2007 *Remote Sensing with Polarimetric Radar* (Hoboken: Wiley-IEEE)

[14] Lee J-S and Pottier E 2009 *Polarimetric Radar Imaging from Basics to Applications* (Boca Raton, FL: CRC Press)

[15] Huynen J R 1970 Phenomenological theory of radar targets *PhD Thesis* University of Technology, Delft, The Netherlands

[16] Voccola K, Cheney M and Yazici B 2012 Polarimetric synthetic-aperture inversion for extended targets in clutter *Inverse Problems* submitted

[17] Migliaccio M, Nunziata F and Gambardella A 2009 On the co-polarized phase difference for oil spill observation *Int. J. Remote Sens.* **30** 1587–602

[18] Schuler D L, Lee J S, Kasilingam D and Pottier E 2004 Measurement of ocean surface slopes and wave spectra using polarimetric SAR image data *Remote Sens. Environ.* **91** 198–211

[19] Merzouki A, McNairn H and Pacheco A 2010 Potential of mapping soil moisture by combining radar backscatter modeling and PolSAR decomposition *IEEE Int. Geosci. Remote Sens. Symp.: IGARSS 2010 (July 2010)* pp 4419–22

[20] Lardeux C, Frison P-L, Tison C, Souyris J-C, Stoll B, Fruneau B and Rudant J-P 2011 Classification of tropical vegetation using multifrequency partial SAR polarimetry *IEEE Geosci. Remote Sens. Lett.* **8** 133–7

[21] Isakov V 1990 *Inverse Source Problems* (*Mathematical Surveys and Monographs* vol 34) (Providence, RI: American Mathematical Society)

[22] Chen H C 1983 *Theory of Electromagnetic Waves: A Coordinate-Free Approach* (New York: McGraw-Hill)

[23] Lekner J 1991 Reflection and refraction by uniaxial crystals *J. Phys: Condens. Matter* **3** 6121–33

[24] Schelkunoff S A 1936 Some equivalence problems of electromagnetics and their application to radiation problems *Bell Syst. Tech. J.* **15** 92–112

[25] Cloude S R and Pottier E 1996 A review of target decomposition theorems in radar polarimetry *IEEE Trans. Geosci. Remote Sens.* **34** 498–518

[26] Smith E M and Tsynkov S V 2011 Dual carrier probing for spaceborne SAR imaging *SIAM J. Imaging Sci.* **4** 501–42